Article

Immunity

Interleukin-2 Activity Can Be Fine Tuned with Engineered Receptor Signaling Clamps

Graphical Abstract

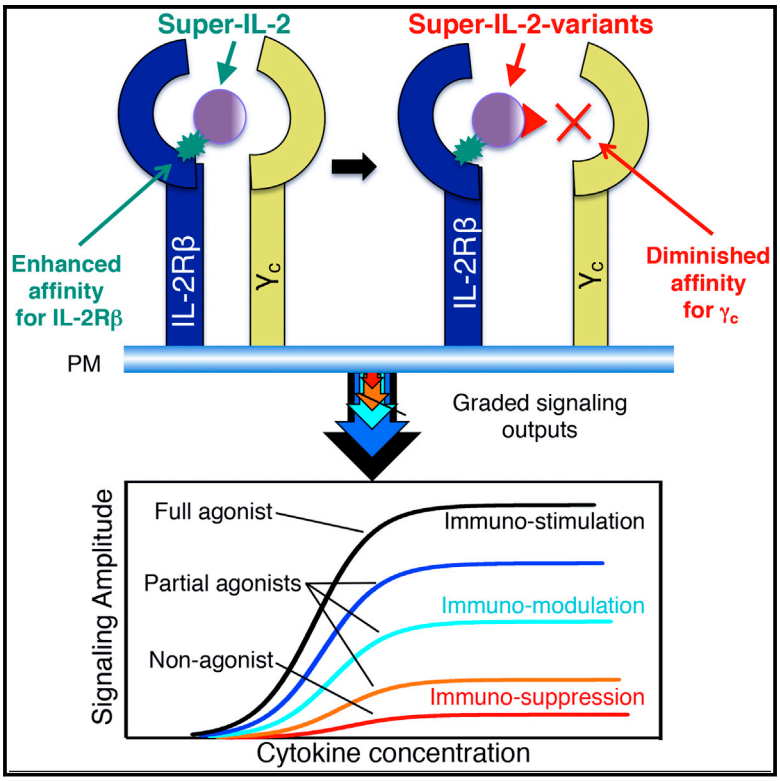

Authors

Suman Mitra, Aaron M. Ring, ..., K. Christopher Garcia, Warren J. Leonard

Correspondence

kcgarcia@stanford.edu (K.C.G.), wjl@helix.nih.gov (W.J.L.)

In Brief

There is resurging interest in controlling the actions of interleukin-2. Leonard, Garcia, and colleagues generated partial agonists of IL-2 with enhanced binding to IL-2Rβ but attenuated γ_c interaction. These reagents yielded a spectrum of signaling amplitudes and biological effects, including the mutein H9-RETR that blocked IL-2- and IL-15-mediated proliferation and cytotoxicity, with therapeutic utility.

Highlights

- Partial IL-2 agonists with altered signaling amplitudes have been created
- A cell's activation state influences its response to particular partial agonists
- One IL-2 mutant, H9-RETR, blocked actions of IL-2 and IL-15, with therapeutic utility
- Our approach should be broadly applicable to many other cytokines

Accession Numbers

GSE64713

Mitra et al., 2015, Immunity *42*, 826–838
May 19, 2015 ©2015 Elsevier Inc.
http://dx.doi.org/10.1016/j.immuni.2015.04.018

Interleukin-2 Activity Can Be Fine Tuned with Engineered Receptor Signaling Clamps

Suman Mitra,[1,7] Aaron M. Ring,[2,7] Shoba Amarnath,[3] Jamie B. Spangler,[2] Peng Li,[1] Wei Ju,[4] Suzanne Fischer,[2] Jangsuk Oh,[1] Rosanne Spolski,[1] Kipp Weiskopf,[5] Holbrook Kohrt,[5] Jason E. Foley,[3] Sumati Rajagopalan,[6] Eric O. Long,[6] Daniel H. Fowler,[3] Thomas A. Waldmann,[4] K. Christopher Garcia,[2,8,*] and Warren J. Leonard[1,8,*]

[1]Laboratory of Molecular Immunology and Immunology Center, National Heart, Lung, and Blood Institute, NIH, Bethesda, MD 20892-1674, USA
[2]Howard Hughes Medical Institute and Department of Molecular and Cellular Physiology and Department of Structural Biology, Stanford University School of Medicine, Stanford, CA 94305, USA
[3]Experimental Transplantation and Immunology Branch, National Cancer Institute, NIH, Bethesda, MD 20892, USA
[4]Lymphoid Malignancies Branch, National Cancer Institute, NIH, Bethesda, MD 20892-1374, USA
[5]Department of Medicine, Division of Oncology, Stanford University School of Medicine, Stanford, CA 94305, USA
[6]Laboratory of Immunogenetics, National Institute of Allergy and Infectious Diseases, NIH, Rockville, MD 20852, USA
[7]Co-first author
[8]Co-senior author
*Correspondence: kcgarcia@stanford.edu (K.C.G.), wjl@helix.nih.gov (W.J.L.)
http://dx.doi.org/10.1016/j.immuni.2015.04.018

SUMMARY

Interleukin-2 (IL-2) regulates lymphocyte function by signaling through heterodimerization of the IL-2Rβ and γ_c receptor subunits. IL-2 is of considerable therapeutic interest, but harnessing its actions in a controllable manner remains a challenge. Previously, we have engineered an IL-2 "superkine" with enhanced affinity for IL-2Rβ. Here, we describe next-generation IL-2 variants that function as "receptor signaling clamps." They retained high affinity for IL-2Rβ, inhibiting binding of endogenous IL-2, but their interaction with γ_c was weakened, attenuating IL-2Rβ-γ_c heterodimerization. These IL-2 analogs acted as partial agonists and differentially affected lymphocytes poised at distinct activation thresholds. Moreover, one variant, H9-RETR, antagonized IL-2 and IL-15 better than blocking antibodies against IL-2Rα or IL-2Rβ. Furthermore, this mutein prolonged survival in a model of graft-versus-host disease and blocked spontaneous proliferation of smoldering adult T cell leukemia (ATL) T cells. This receptor-clamping approach might be a general mechanism-based strategy for engineering cytokine partial agonists for therapeutic immunomodulation.

INTRODUCTION

Interleukin-2 (IL-2) is a four α-helical bundle type I cytokine (Boyman and Sprent, 2012; Cheng et al., 2011; Liao et al., 2013; Rochman et al., 2009) that signals through heterodimerization of the IL-2Rβ and the IL-2Rγ (now known as the common cytokine receptor γ chain, γ_c) receptor subunits (Nakamura et al., 1994; Nelson et al., 1994). Discovered as T cell growth factor (Morgan et al., 1976), IL-2 is a pleiotropic cytokine that also modulates the differentiation of T helper cells (Laurence et al., 2007; Liao et al., 2008, 2011; Zhu et al., 2010), promotes regulatory T (Treg) cell development (Cheng et al., 2011; Yu et al., 2009), augments cytolytic activity of natural killer and lymphokine-activated killer cells (Liao et al., 2013), mediates activation-induced cell death (AICD) (Lenardo, 1991), and regulates effector versus memory $CD8^+$ T cell generation (Kalia et al., 2010; Pipkin et al., 2010).

On resting lymphocytes, IL-2 signals via intermediate-affinity receptors ($K_d \sim 10^{-9}$ M) consisting of IL-2Rβ and γ_c, whereas activated lymphocytes and Treg cells additionally express IL-2Rα, which combines with IL-2Rβ and γ_c to form high-affinity receptors ($K_d \sim 10^{-11}$ M) (Cheng et al., 2011; Liao et al., 2013). Whereas γ_c is shared by the receptors for IL-4, IL-7, IL-9, IL-15, and IL-21 (Rochman et al., 2009) and is encoded by the gene mutated in humans with X-linked severe combined immunodeficiency (Noguchi et al., 1993), IL-2Rβ is shared by the receptor for IL-15 (Waldmann, 2006), a cytokine critical for normal development of NK cells and memory $CD8^+$ T cells (Waldmann, 2006). Analogous to IL-2Rα, IL-15 also has a sushi-domain-containing third subunit, IL-15Rα (Rochman et al., 2009; Waldmann, 2006). IL-2 signals via three principal signaling pathways, the JAK-STAT pathway (mainly activating JAK1, JAK3, STAT5A, and STAT5B), the RAS-MAP kinase pathways, and the PI 3-kinase-AKT pathway (Kim et al., 2006), which together contribute to the range of biological actions mediated by IL-2 (Liao et al., 2013).

IL-2 can induce the expansion of T cells to enhance adoptive immunotherapy and is approved by the FDA for the treatment of melanoma and renal cell carcinoma, with complete remission in a subset of patients (Rosenberg, 2014). However, IL-2 can also promote pathologic responses, and a therapeutic goal is to maintain the desired actions of this cytokine while blocking untoward deleterious responses. Blocking IL-2 can also be efficacious, and two monoclonal antibodies (mAbs) to human IL-2Rα, Daclizumab and Basiliximab, are approved by the FDA, with utility in preventing, for example, renal (Vincenti et al., 1998) and cardiac (Beniaminovitz et al., 2000; Hershberger et al., 2005) transplantation rejection and in treating multiple sclerosis (Bielekova et al., 2004; Gold et al., 2013). However, these antibodies cannot block IL-2 signaling via intermediate-affinity IL-2Rβ-γ_c receptors expressed on NK and memory $CD8^+$

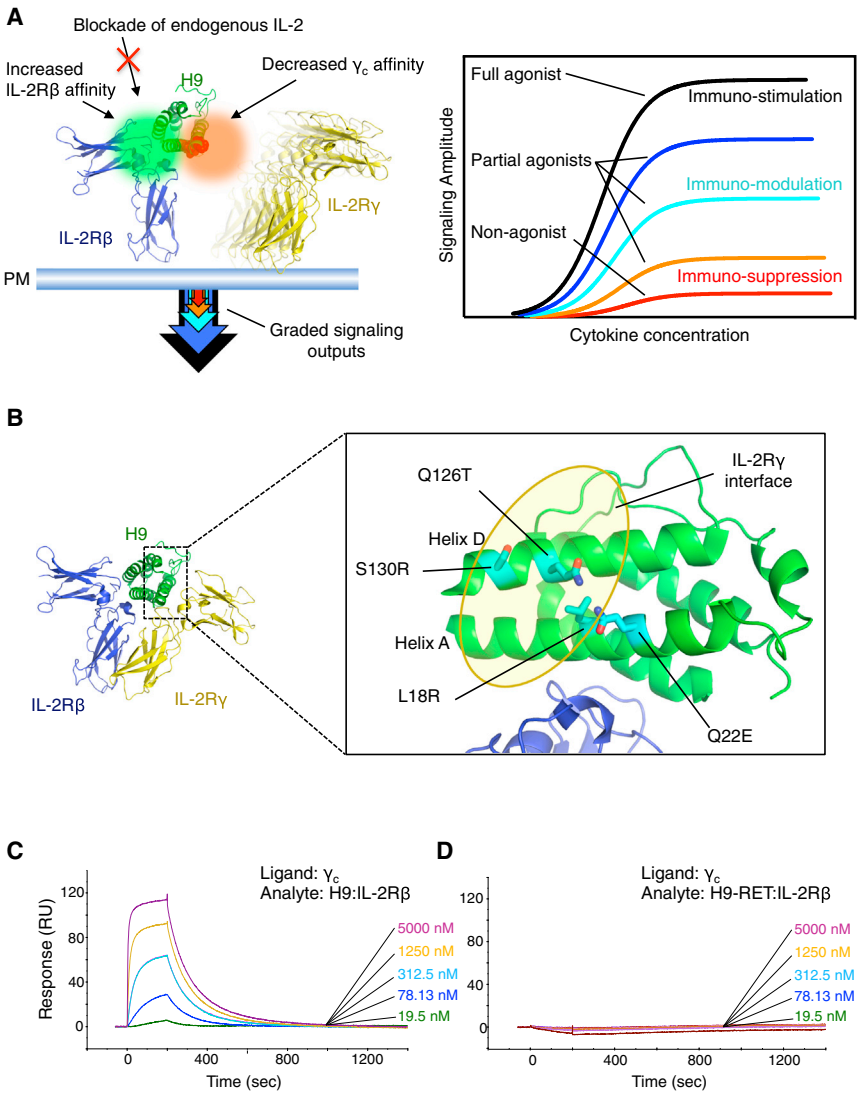

Figure 1. Generation of Mechanism-Based IL-2 Variants by Disrupting γ_c Binding.

(A) Left: The green region indicates the changes in IL-2 used to generate H9 "super-IL-2" with high-affinity binding to IL-2Rβ (Levin et al., 2012), thus blocking the binding of endogenous IL-2 (indicated by the red "X"). The red circle indicates changes in H9 that decrease binding to γ_c and thus IL-2Rβ-γ_c heterodimerization. Right: Depending on the degree of disruption of γ_c binding, different activity potency and function should be generated, as indicated.

(B) Structure of the H9-IL-2Rβ-γ_c complex (H9 is green; IL-2Rβ is blue; γ_c is gold). The mutations (L18R, Q22E, Q126T, and S130R) incorporated into H9-RETR to disrupt the interaction of IL-2 with γ_c are shown in cyan (right).

(C and D) Surface plasmon resonance analysis of the binding of H9-IL-2Rβ (C) and H9-RET-IL-2Rβ (D) complexes to γ_c.

T cells. Although anti-human IL-2Rβ mAb Mikβ1 can block *trans*-presentation of IL-2 and IL-15 to cells expressing IL-2Rβ-γ_c receptors (Morris et al., 2006), it is relatively ineffective in blocking *cis*-signaling by IL-2 or IL-15 via their high-affinity heterotrimeric receptors (Morris et al., 2006; Waldmann et al., 2013).

We have previously used the structure of the high-affinity IL-2-IL-2R complex (Rickert et al., 2005; Wang et al., 2005) to develop IL-2 "superkines" with augmented action due to enhanced binding affinity for IL-2Rβ, which eliminates the functional requirement for IL-2Rα (Levin et al., 2012). We now have used this super-IL-2 platform to generate mutants that retain increased binding affinity for IL-2Rβ but that exhibited decreased binding to γ_c and thereby defective IL-2Rβ-γ_c heterodimerization and signaling. These are mechanism-based IL-2 partial agonists that can act as IL-2-receptor-signaling "clamps" and allow fine tuning of the signaling amplitude. We have characterized the signaling effects and patterns of gene induction induced by these IL-2 variants as well as their functional effects. One of these partial agonists, H9-RETR, was a potent antagonist of both IL-2 and IL-15 signaling and function in vitro, inhibiting T cell proliferation and NK cytolytic activity. Moreover, it inhibited spontaneous proliferation of smoldering adult T cell leukemia (ATL) T cells ex vivo and was superior to blocking antibodies against IL-2Rα and IL-2Rβ. Furthermore, a stabilized Fc-fusion version of H9-RETR prolonged survival in a murine model of graft-versus-host disease after allogeneic bone-marrow transplantation.

RESULTS

Partial IL-2 Agonists Can Be Engineered as IL-2 Receptor Signaling "Clamps"

In order to elucidate the signaling and biological actions of IL-2 as well as to create molecules with therapeutic potential, we sought to create next-generation analogs of IL-2 with diminished or absent signaling amplitudes. We hypothesized that it would be possible to "clamp" IL-2 signaling strength in a manner that is relatively insensitive to ligand concentration and that this might controllably offer the ability to modulate IL-2 signaling to varying degrees. We speculated that IL-2 "superkines" with augmented action due to enhanced binding affinity for IL-2Rβ (Levin et al., 2012) could serve as a dominant-negative scaffold to create a "receptor signaling clamp" to block endogenous signaling. Directed mutation to diminish binding to γ_c would then attenuate IL-2Rβ-γ_c heterodimerization and represent a class of mechanism-based IL-2 partial agonists and non-signaling (neutral) molecules that act as antagonists (see schematic in Figure 1A). Based on the human IL-2-IL-2R crystal structure (Wang et al., 2005) and structure-function studies with mouse IL-2 (Zurawski et al., 1993), we identified four key residues at the human IL-2-γ_c interface (Figure 1B) and generated H9 variants containing one (Q126T), two (L18R, Q22E), three (L18R, Q22E, and Q126T), or four (L18R, Q22E, Q126T, and S130R) mutations

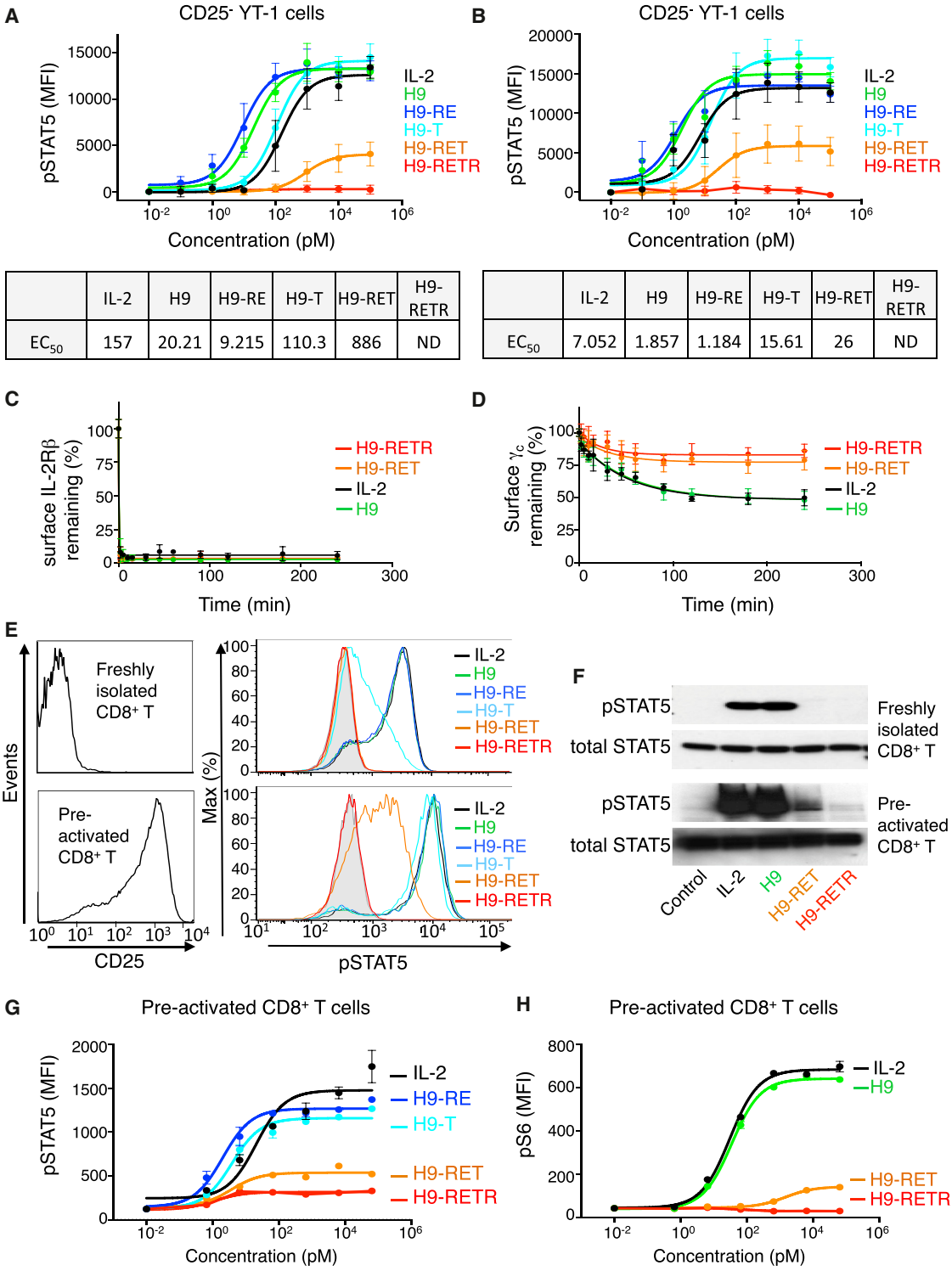

	IL-2	H9	H9-RE	H9-T	H9-RET	H9-RETR
EC_{50}	157	20.21	9.215	110.3	886	ND

	IL-2	H9	H9-RE	H9-T	H9-RET	H9-RETR
EC_{50}	7.052	1.857	1.184	15.61	26	ND

Figure 2. Attenuated Signaling by IL-2 Variants

(A and B) Wild-type IL-2 or the indicated H9 variants were assayed for their ability to induce STAT5 phosphorylation in $CD25^-$ (A) and $CD25^+$ (B) YT-1 human NK-like cells. The EC_{50} values are indicated below the panels.

(C and D) Internalization kinetics of IL-2Rβ (C) and γ_c (D) relative to maximal surface expression in $CD25^-$ YT-1 cells after stimulation with the indicated IL-2 variants.

(E) Freshly isolated human $CD8^+$ T cells (top) or $CD8^+$ T cells pre-activated with anti-CD3 + anti-CD28 (bottom) were left unstimulated or stimulated with 1 μg/ml IL-2, H9, H9-RE, H9-T, H9-RET, or H9-RETR for 30 min. CD25 expression (left) or pSTAT5 (right) were assayed by flow cytometry.

(legend continued on next page)

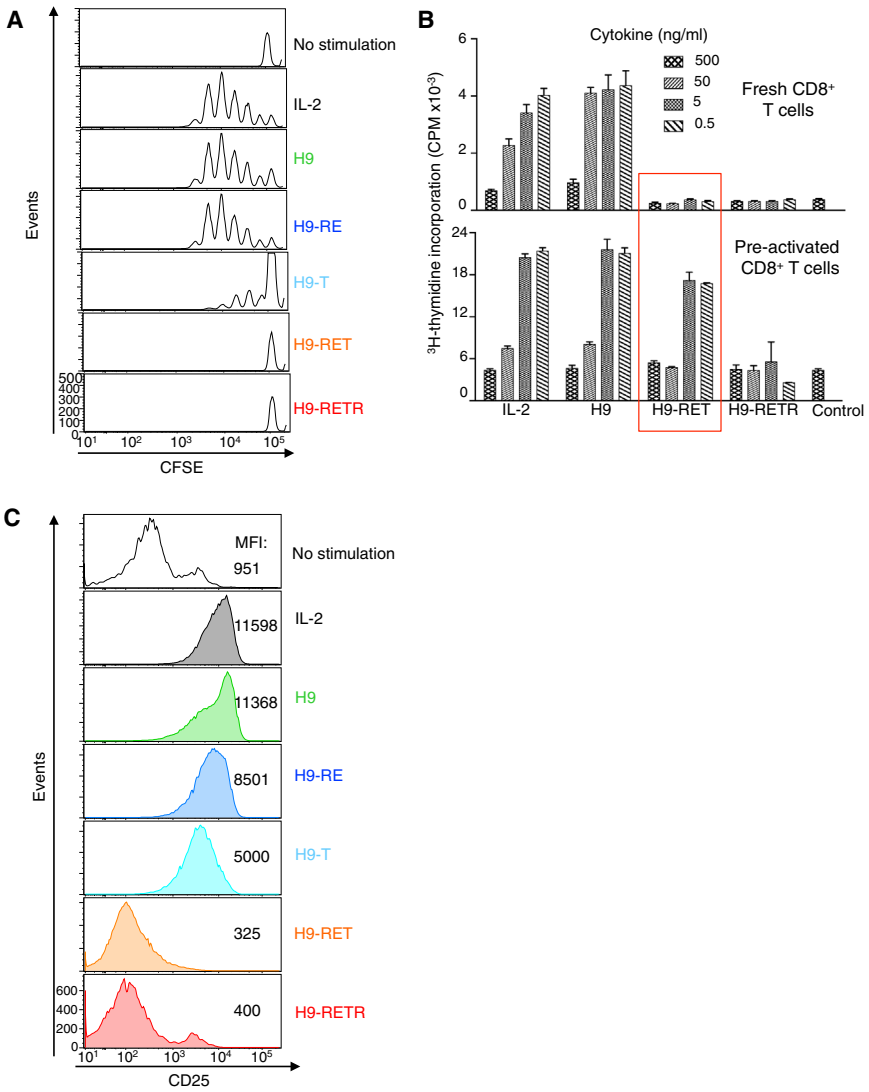

Figure 3. Graded IL-2 Signaling Strength Exerted by the IL-2 Analogs Can Differentially Affect Lymphocyte Proliferation and Cellular Activation

(A) Proliferation in response to IL-2, H9, H9-RE, H9-T, H9-RET, and H9-RETR. Induction of proliferation of freshly isolated human CD8$^+$ T cells by IL-2 and H9 but not by H9-RET or H9-RETR, with intermediate effects of H9-T. Cells were labeled with CFSE and stimulated with the indicated IL-2 variants, and CFSE dilution was assessed by flow cytometry 5 days later.

(B) Freshly isolated human CD8$^+$ T cells and CD8$^+$ T cells pre-activated with anti-CD3 + anti-CD28 were cultured in 96-well plates with varying concentrations of the indicated IL-2 variants for 2 days and [^{3}H]thymidine incorporation measured. Bars represent mean ± SEM. Cells were combined from two donors. Data are representative of two independent experiments performed in triplicate.

(C) CD25 expression on CD8$^+$ T cells pre-activated with anti-CD3 + anti-CD28 and then treated with IL-2, H9, H9-RE, H9-T, H9-RET, or H9-RETR. Data are representative of three independent experiments. MFIs are indicated.

(denoted as H9-T, H9-RE, H9-RET, and H9-RETR, respectively, based on the newly introduced amino acids). By surface plasmon resonance, recombinant H9 and H9-RET proteins had similar affinities for IL-2Rβ, but whereas the H9-IL-2Rβ complex efficiently bound γ_c (Figure 1C), H9-RET-IL-2Rβ did not (Figure 1D).

IL-2 Signaling Strength Inversely Correlates with the Degree of Mutation at the γ_c Interface

To determine the activity of the H9 variants, we purified CD25$^+$ and CD25$^-$ subpopulations of NK-like YT-1 cells and quantified signaling. The H9 mutants behaved as IL-2 partial agonists, producing a range of signaling efficacies from >90% down to <10% of the wild-type E_{max} (maximum possible effect) of phosphorylation of STAT5 (Figures 2A and 2B), with the activity for each analog inversely correlating with the degree of mutation at the γ_c interface. Signaling potency was relatively independent of IL-2Rα, as demonstrated by the relative E_{max} values for the H9 variants on CD25$^-$ (Figure 2A) versus CD25$^+$ (Figure 2B) YT-1 cells, suggesting that altered binding to γ_c was primarily responsible for the behavior of the H9 variants. H9-RET and H9-RETR also exhibited diminished induction of other IL-2 signaling pathways, including pERK1-pERK2 in CD25$^-$ and CD25$^+$ YT-1 cells (Figures S1A and S1B). Moreover, IL-2 induces internalization of IL-2Rβ and γ_c (Hémar et al., 1995), but whereas both H9-RET and H9-RETR drove rapid and complete IL-2Rβ internalization analogous to IL-2 and H9 (Figure 2C), they were much less efficient in driving internalization of γ_c (Figure 2D), consistent with their diminished binding to γ_c. Thus, variably disrupting the γ_c-binding interface of H9 can yield a variety of IL-2 partial agonists, potentially with a range of signaling efficacies.

We next analyzed these molecules by utilizing primary cells, and neither H9-RET nor H9-RETR could induce pSTAT5 in freshly isolated human CD8$^+$ T cells (Figures 2E and 2F, top), which express less IL-2Rβ and γ_c than activated CD8$^+$ T cells (Figure S1C, upper versus lower) and little or no IL-2Rα (Figure 2E, left top). However, after activation of CD8$^+$ T cells with anti-CD3 + anti-CD28, although H9-RETR remained essentially inert, H9-RET

(F) Cells were treated with IL-2, H9, H9-RET, or H9-RETR, lysed, and immunoblotted with antibodies to pSTAT5 or total STAT5.

(G) Dose-response curves of pSTAT5 induced by IL-2, H9-RE, H9-T, H9-RET, and H9-RETR.

(H) Dose-response curves of phospho-S6 ribosomal protein (pS6) by IL-2, H9, H9-RET, and H9-RETR.

For dose-response experiments (A, B, G, H), the abscissa indicates the log of cytokine concentration in ng/ml. MFI, mean fluorescent intensity. Data are representative of at least two experiments per panel (error bars, SEM of triplicates). See also Figure S1.

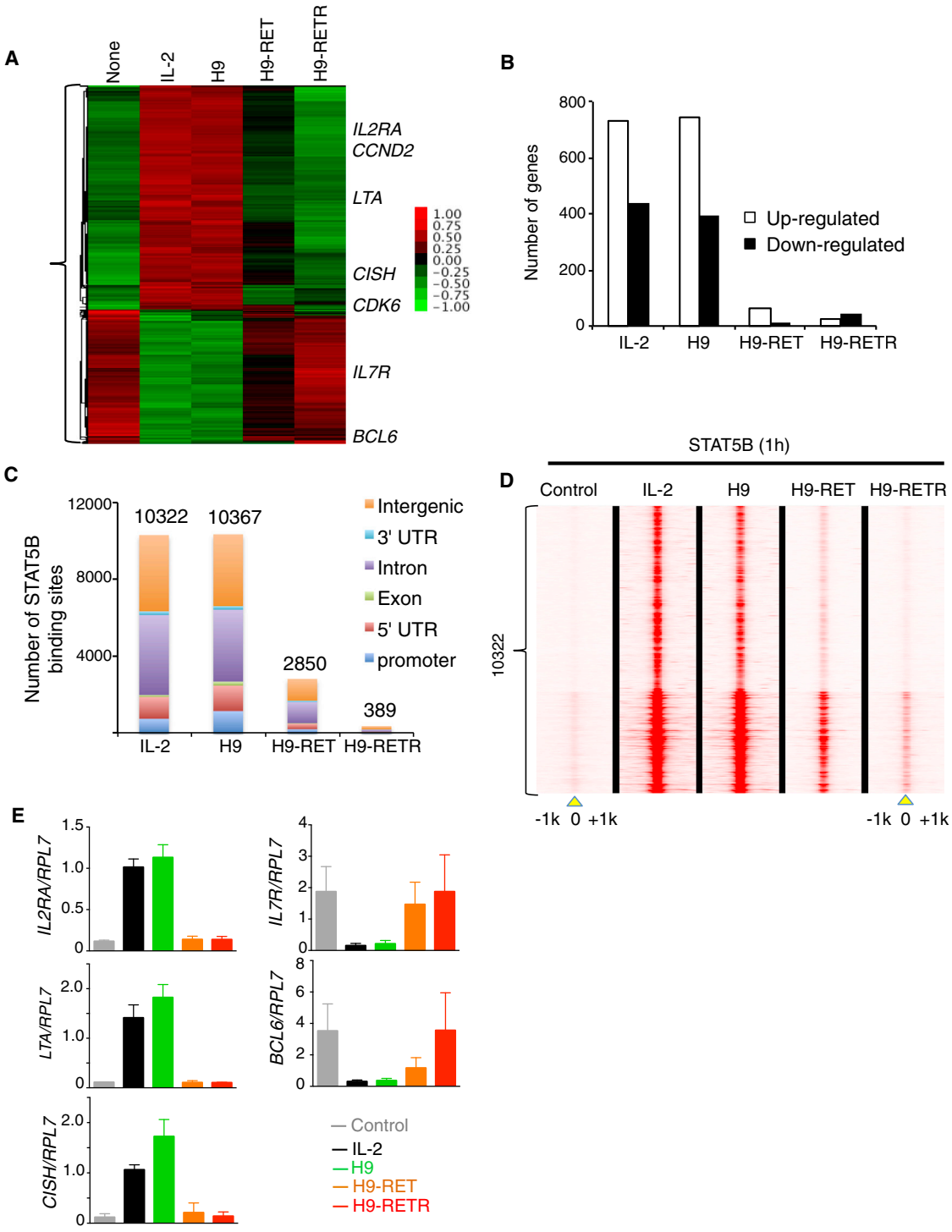

Figure 4. Comparison of Global STAT5 Binding and Gene Expression Profiles of IL-2 versus IL-2 Analogs

(A) RNA-seq heat map analysis of human CD8$^+$ T cells pre-activated with anti-CD3 + anti-CD28 and then treated with IL-2, H9, H9-RET, and H9-RETR (1 μg/ml) for 24 hr. Shown are the genes whose expression in the treated samples were at least twice (red) or less than half (green) that found in the control (expression of each gene was normalized between −1.00 and 1.00 according to the color scale).

(B) Number of mRNAs upregulated (open bars) or downregulated (solid bars) after stimulation with indicated cytokines. IL-2, H9, H9-RET, and H9-RETR, respectively, induced 731, 742, 65, and 23 mRNAs and repressed 437, 397, 13, and 46 mRNAs (fold change ≥ 2; p value < 1×10^{-10}).

(C) Number of STAT5B binding sites in CD8$^+$ T cells pre-activated with anti-CD3 + anti-CD28 and then treated with the IL-2 variants based on ChIP-seq data and their genome-wide distribution. Shown are 5′ untranslated regions (5′ UTR), exons, introns, and 3′ untranslated regions (3′ UTR) as defined in human RefSeq database assembly GRCh37.p9. 5 kb upstream of TSS was designated as the promoter region.

(legend continued on next page)

induced partial phosphorylation of STAT5 (Figure 2E, bottom right; Figure 2F, bottom; Figure 2G) and S6 ribosomal protein (Figure 2H). H9-T induced low pSTAT5 in freshly isolated $CD8^+$ T cells (Figure 2E, top right), and this was markedly increased in $CD8^+$ T cells pre-activated with anti-CD3 + anti-CD28, albeit still not up to the amount of pSTAT5 observed with IL-2, H9, or H9-RE (Figure 2E, bottom right and Figure 2G). Thus, H9-T and H9-RET exhibit intermediate activities typical of partial agonists.

Differential Effects on Proliferation Depending on the Activation State of the Cells

Given the weak pSTAT5 expression induced by H9-RET and H9-RETR, we next investigated their effects on proliferation. Whereas IL-2, H9, and H9-RE strongly induced proliferation of primary human $CD8^+$ T cells and H9-T was intermediate in its effects, neither H9-RET nor H9-RETR induced proliferation of these cells as assessed by carboxyfluorescein diacetate succinimidyl diester (CFSE) dilution (Figure 3A) or by [^{3}H]thymidine incorporation (Figure 3B, top). However, when $CD8^+$ T cells were pre-activated with anti-CD3 + anti-CD28, H9-RETR still had no effect, but H9-RET reproducibly induced proliferation (Figure 3B, bottom). Thus, H9-RET induces different functional outcomes in distinct cell subsets, analogous to its differential effects on pSTAT5 in freshly isolated $CD8^+$ T cells versus $CD8^+$ T cells pre-activated with anti-CD3 + anti-CD28 (Figure 2E). As expected, IL-2 and H9 potently induced IL-2Rα expression in $CD8^+$ T cells pre-activated with anti-CD3 + anti-CD28, H9-RE and H9-T were intermediate in their IL-2Rα induction, but H9-RET and H9-RETR decreased IL-2Rα expression, actually to below the control (Figure 3C), presumably reflecting their competing with endogenous IL-2.

Attenuation of Gene Expression by H9-RET and H9-RETR Correlates with Defective STAT5 Activation

We next used RNA-seq to further elucidate the basis for the actions of IL-2 and H9 versus H9-RET and H9-RETR in human $CD8^+$ T cells pre-activated with anti-CD3 + anti-CD28 (Figures 4A and 4B). As expected, IL-2 and H9 induced genes that control cell cycle or are involved in cytokine signaling (e.g., *IL2RA*, *CCND2*, *CISH*, and *CDK6*) but repressed many other genes (e.g., *IL7R*, *BCL6*), whereas H9-RET had only weak stimulatory activity and H9-RETR had almost no effect (Figure 4A and Table S1), revealing quantitative and qualitative differences in gene expression induced by full and partial agonists. IL-2 and H9 induced more genes than they repressed, whereas H9-RETR repressed more genes than it induced, although its overall effect was minimal (Figure 4B). Because STAT5 is a key mediator of IL-2-induced transcription, we used chromatin immunoprecipitation coupled to next generation sequencing (ChIP-seq) to globally evaluate genomic STAT5 binding. H9-RET and H9-RETR induced STAT5 binding to consensus 5′-TTCnnnGAA-3′ motifs, but at far fewer sites than observed with either IL-2 or H9 (Figure 4C). Based on heat map clustering, only ~35% of IL-2-induced STAT5 sites were also induced by H9-RET, whereas H9-RETR had little effect (Figure 4D). The induction (*IL2RA*, *LTA*, *CISH*) or repression (*IL7R*, *BCL6*) of several STAT5 target genes by IL-2 and H9 in $CD8^+$ T cells pre-activated with anti-CD3 + anti-CD28 was confirmed by RT-PCR (Figure 4E), whereas neither H9-RET nor H9-RETR had an effect, except that interestingly, unlike RETR, RET reproducibly lowered *BCL6* expression (Figure 4E), indicating that the H9-RET partial agonist induces a sufficient signal to mediate partial repression of this gene, whereas H9-RETR did not, again indicating distinctive behavior by these molecules.

H9-RETR Potently Blocks Cytokine Signaling and NK Cell Activity with Efficacy Similar or Greater than that of Blocking Antibodies to IL-2Rα and IL-2Rβ

The above studies established the attenuated activity of H9-RET and negligible activity of H9-RETR, which effectively is a dominant-negative antagonist of IL-2. Given their enhanced binding to IL-2Rβ and ability to decrease IL-2Rα expression on $CD8^+$ T cells pre-activated with anti-CD3 + anti-CD28, we hypothesized that these molecules would inhibit not only endogenous IL-2, but also IL-15, which also signals via IL-2Rβ and γ_c. Indeed, both H9-RET and H9-RETR inhibited IL-2-induced (Figure 5A) and IL-15-induced (Figure 5B) pSTAT5 in $CD8^+$ T cells, with H9-RETR being more potent. This inhibition correlated with the ability of H9-RET and H9-RETR to lower T cell receptor (TCR)-induced (Figure 3C) and IL-2-induced (Figure S2A) CD25 expression to below the expression observed in unstimulated control cells. Correspondingly, in human $CD8^+$ T cells pre-activated with anti-CD3 + anti-CD28, H9-RET and H9-RETR inhibited IL-2-induced proliferation (Figure S2B, left), with corresponding effects on IL-15-induced proliferation as well (Figure S2B, right). We speculated that H9-RET and H9-RETR would also inhibit TCR-induced proliferation, which depends on IL-2, and this was indeed the case (Figure S2C) and correlated with decreased CD25 expression (Figure S2D). Similarly, in contrast to IL-2, which promotes Th1, Th9, and Treg cell differentiation but inhibits Th17 cell differentiation (Liao et al., 2013), H9-RET and H9-RETR inhibited Th1, Th9, and Treg cell differentiation but augmented Th17 cell differentiation (Figure S2E), underscoring their ability to potently antagonize IL-2. The activation of primary human NK cells by IL-2 was also potently blocked by H9-RETR, as measured by IL-2-induced CD69 expression (Figure 5C), and cytotoxicity toward the breast cancer cell line HER18 (Figure 5D) and the chronic myelogenous leukemia cell line K562 (Figure 5E) were also inhibited by H9-RETR. Neither H9-RET nor H9-RETR stimulated CD69 expression (Figure 5C) or cytotoxicity by primary NK cells (Figure 5D).

Given H9-RETR's effectiveness as an IL-2 and IL-15 antagonist in vitro, we wished to investigate its ability to antagonize

(D) IL-2-induced STAT5B peaks at 1 hr of stimulation were used to perform heat map clustering centered ~1 kb upstream and ~1 kb downstream of the STAT "peak summit" (indicated by position "0"). The strength of binding induced by IL-2, H9, H9-RET, and H9-RETR is indicated by the intensity of red. 10322 (y axis) is the number of IL-2-induced STAT5B binding sites.

(E) Expression of *IL2RA*, *LTA*, *CISH*, *IL7R*, and *BCL6* RNA relative to *RPL7* in human $CD8^+$ T cells pre-activated with anti-CD3 + anti-CD28 left unstimulated or stimulated with IL-2, H9, H9-RET, and H9-RETR for 24 hr. Data are representative of at least two experiments, except for the RNA-seq experiment, in which select genes were confirmed by RT-PCR. Shown is mean ± SEM.

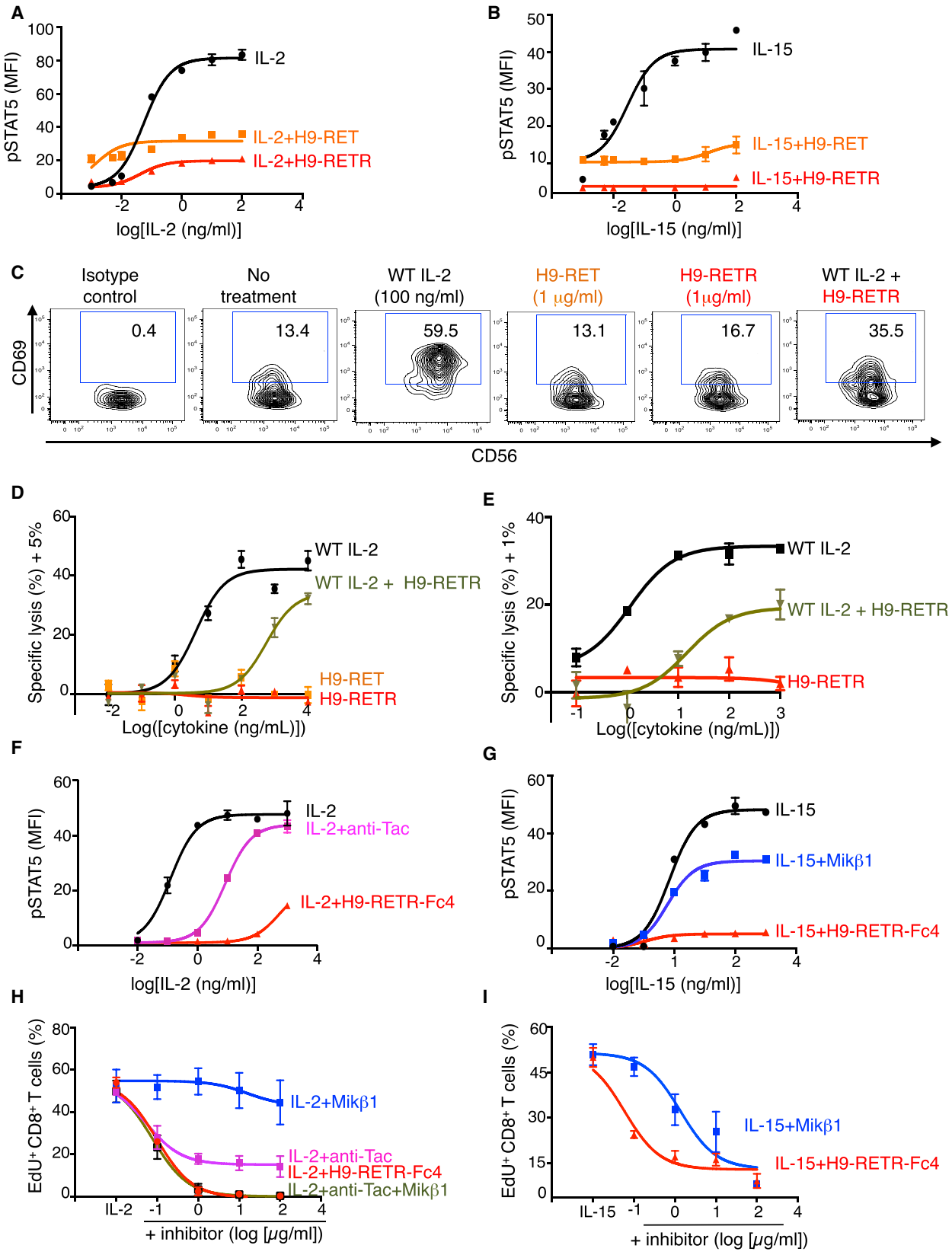

(legend on next page)

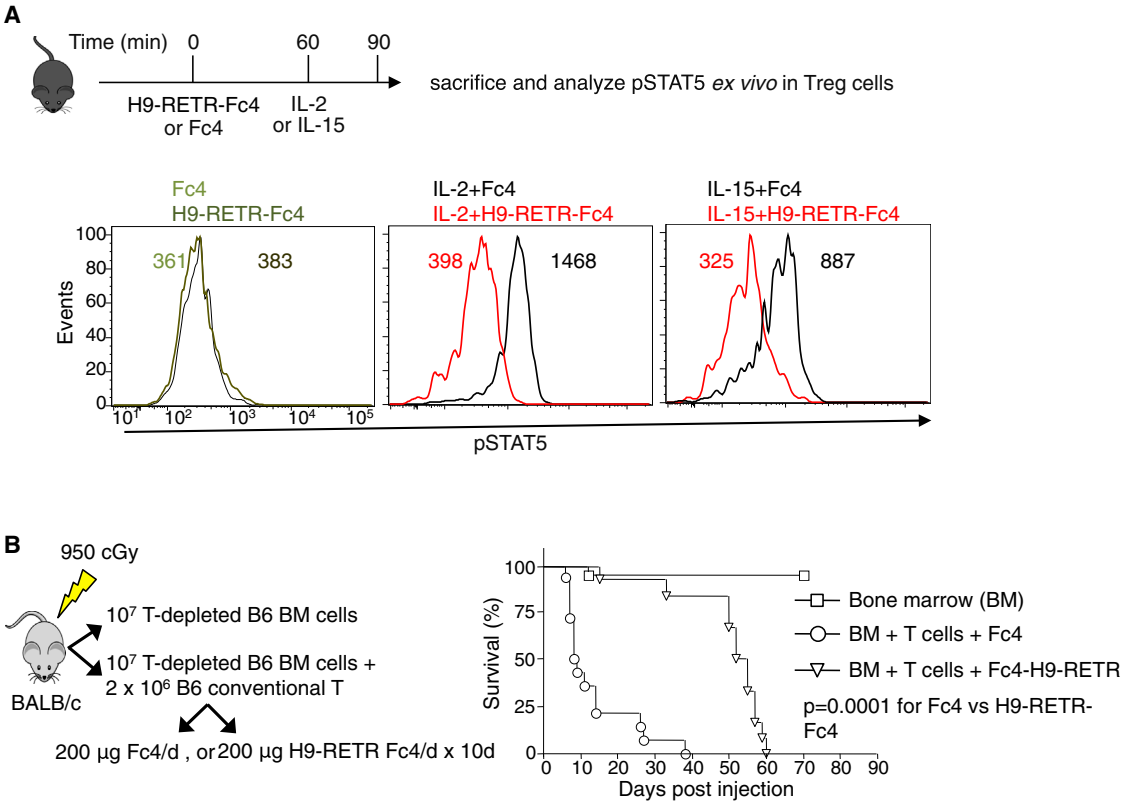

Figure 6. In Vivo Efficacy of the Mechanism-Based IL-2 Antagonist, H9-RETR

(A) H9-RETR inhibits IL-2-induced (middle) and IL-15-induced (right) STAT5 phosphorylation in vivo. C57BL/6 mice were injected (i.p.) with Fc4 (100 µg) or H9-RETR-Fc4 (100 µg) 60 min prior to IL-2 or IL-15 (2 µg). Schematic of the protocol for the experiment is shown. pSTAT5 was measured 30 min later in splenic $CD4^+CD25^+FoxP3^+$ T cells. MFIs are indicated. Data are representative of three independent experiments.

(B) H9-RETR-Fc4 attenuates GVHD. BALB/c mice were irradiated (950 cGy) and transplanted with 10 million T-cell-depleted bone marrow (BM) cells without or with 2 million Treg-cell-depleted pan-T cells from C57BL/6 mice. Mice receiving pan-T cells were treated with Fc4 or H9-RETR-Fc4 fusion protein by i.p. injections for 10 days with 100 µg/dose twice a day. Data represent survival curves pooled from three independent experiments and analyzed using the Kaplan-Meier method and the log-rank test. p = 0.0001 for Fc4 versus H9-RETR-Fc4.

See also Figure S3.

endogenous cytokines in vivo. Because IL-2 has a short serum half-life (Donohue and Rosenberg, 1983), we fused H9-RETR to the Fc fragment of human IgG4 (Fc4), an isotype with diminished antibody-dependent cellular cytotoxicity (ADCC) and antibody-dependent cellular phagocytosis (ADCP) (Strohl, 2009). When tested in vitro, as compared to anti-Tac mAb to CD25 and Mikβ1 mAb to IL-2Rβ (Morris et al., 2006), H9-RETR-Fc4 more potently blocked IL-2-mediated (Figure 5F) and IL-15-mediated (Figure 5G) pSTAT5 induction in $CD8^+$ T cells pre-activated with anti-CD3 + anti-CD28 and inhibited IL-2-induced (Figure 5H) and IL-15-induced (Figure 5I) proliferation of human $CD8^+$ T cells. Moreover, H9-RETR-Fc4 was as effective as the combination of anti-Tac and Mikβ1 in blocking IL-2 proliferation (Figure 5H) and more potent than Mikβ1 in inhibiting IL-15-induced proliferation (Figure 5I).

Figure 5. H9-RETR Potently Inhibits IL-2R-Mediated Signaling

(A and B) H9-RET and H9-RETR are competitive inhibitors of IL-2 (A) and IL-15 (B). Human $CD8^+$ T cells pre-activated with anti-CD3 + anti-CD28 were incubated with the indicated concentrations of IL-2 or IL-15 in the absence or presence of 1 µg/ml of H9-RET or H9-RETR.

(C–E) H9-RETR blocks IL-2-induced NK cell activation and cytotoxicity.

(C) Unlike IL-2, neither H9-RET nor H9-RETR (1 µg/ml) stimulated CD69 expression in primary human NK cells after incubation for 24 hr, but H9-RETR inhibited IL-2 (100 ng/ml)-induced CD69 expression. The experiment was performed twice.

(D and E) Neither H9-RET nor H9-RETR stimulated cytotoxicity in primary human NK cells, and H9-RETR at 10^3 ng/ml inhibited IL-2-induced NK cell cytotoxicity of HER18 (D) and K562 (E) target cells. NK cells and target cells were incubated at a 10:1 ratio for 4 hr in the presence of the indicated cytokines. HER18 cell lysis was determined by ^{51}Cr release and performed in triplicate; lysis of K562 cells was assessed by flow cytometry. Four independent experiments were performed.

(F and G) H9-RETR more potently blocks IL-2-induced (F) and IL-15-induced (G) STAT5 phosphorylation than anti-Tac or Mikβ1 mAbs in human $CD8^+$ T cells pre-activated with anti-CD3 + anti-CD28.

(H and I) H9-RETR more potently inhibits IL-2-induced (H) or IL-15-induced (I) proliferation than anti-Tac or Mikβ1.

Shown are means ± SEM. Data are representative of three independent experiments. See also Figure S2.

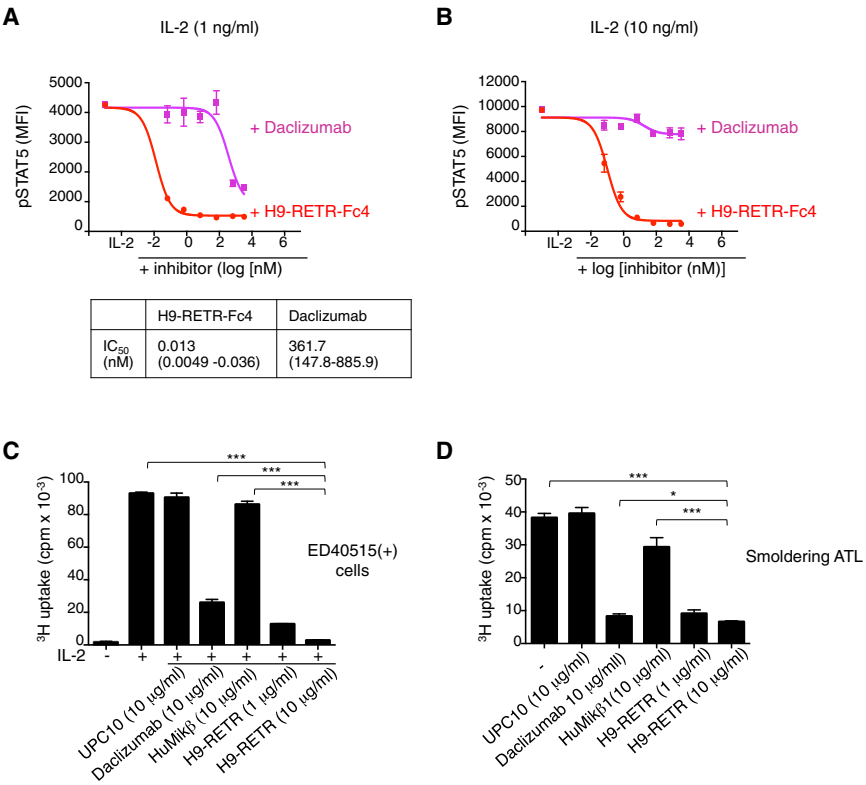

	H9-RETR-Fc4	Daclizumab
IC_{50} (nM)	0.013 (0.0049 -0.036)	361.7 (147.8-885.9)

Figure 7. H9-RETR Potently Inhibits IL-2-Induced pSTAT5 Signaling and the Proliferation of Smoldering ATL Cells

(A and B) Dose-response effect of increasing concentration of H9-RETR-Fc4-fusion protein versus daclizumab on IL-2-induced pSTAT5 in human $CD8^+$ T cells pre-activated with anti-CD3 + anti-CD28. $CD8^+$ T cells were pre-activated with anti-CD3 and anti-CD28 and cultured as described in the Experimental Procedures and incubated with the indicated concentration of H9-RETR-Fc4 or daclizumab for 30 min, re-stimulated with 1 ng/ml (A) or 10 ng/ml (B) IL-2 for 20 min, and pSTAT5 was measured by flow cytometry. Data are representative of two independent experiments. The IC_{50} values for H9-RETR-Fc4 and daclizumab are indicated below (A).

(C) Blocking of proliferation of ED40515(+) T cells cultured with 50 U/ml IL-2 for 3 days in the presence or absence of UPC10 (a murine IgG2a monoclonal antibody that does not recognize resting or activated human blood lymphocytes), daclizumab, Mikβ1, or H9-RETR, as indicated. Data are representative of two experiments, each performed in triplicate.

(D) Spontaneous 6 day proliferation assay of cells from a patient with smoldering ATL, treated with UPC10, daclizumab, Mikβ1, or H9-RETR. Assays were performed in triplicate. *$p < 0.05$; ***$p < 0.001$.

Shown are means ± SEM.

Potent Inhibitory Actions of H9-RETR In Vivo

We next evaluated H9-RETR-Fc4 in vivo. Under steady-state conditions, Treg cells are the dominant population of primary cells expressing high-affinity IL-2 receptors (Boyman and Sprent, 2012; Cheng et al., 2011; Liao et al., 2013; Littman and Rudensky, 2010) and can act as a systemic "barometer" of IL-2 signaling. Pre-treating mice with H9-RETR-Fc4 for 60 min prior to administering IL-2 or IL-15 inhibited phosphorylation of STAT5 in $CD4^+FoxP3^+$ Treg cells, as assessed ex vivo (Figure 6A). Next, we tested the relative efficacy of H9-RETR-Fc4 versus anti-IL-2Rα mAb (clone PC61) in blocking IL-2 signaling in vivo (Figure S3) and found that H9-RETR-Fc4 was more effective in blocking IL-2-induced pSTAT5 signaling in Treg cells. These data demonstrated in vivo potential of H9-RETR-Fc4 as a potent IL-2 antagonist. Because IL-2 and IL-15 signaling contributes to acute graft-versus-host disease (GVHD) in experimental murine models (Blaser et al., 2005; Chinen and Buckley, 2010; Ferrara et al., 1986), we hypothesized that H9-RETR-Fc4 might inhibit lethal GVHD in a T-cell-mediated C57BL/6-into-BALB/C model of fully-MHC mismatched bone marrow transplantation. Indeed, mice treated for 10 days with H9-RETR-Fc4 had longer survival than mice receiving control Fc4 protein (Figure 6B).

H9-RETR Potently Blocks IL-2 Signaling and Inhibits the Spontaneous Proliferation of Smoldering Adult T Cell Leukemia Cells

We next compared the inhibitory potency of H9-RETR-Fc4 with daclizumab and found that H9-RETR-Fc4 was more potent in blocking IL-2-induced phosphorylation of STAT5 in $CD8^+$ T cells pre-activated with anti-CD3 + anti-CD28 (Figures 7A and 7B). However, daclizumab had little effect on signaling in response to high-dose IL-2 (10 ng/ml), a dose capable of titrating intermediate-affinity receptors (Figure 7B). These results underscore the inhibitory potency of H9-RETR-Fc4.

Human T cell lymphotropic virus-I (HTLV-I) causes adult T cell leukemia (ATL), a malignant expansion of $CD4^+$ T cells that exhibits an early growth phase that involves autocrine signals by IL-2 and IL-15 and paracrine signals by IL-9. Such cytokine-dependent proliferation occurs in patients with chronic and smoldering but not acute ATL (Ju et al., 2011). To test the efficacy of H9-RETR in ATL, we first used ATL-derived ED40515 cells, and H9-RETR potently inhibited IL-2-induced proliferation of these cells and was superior to either daclizumab or Mikβ1 (Figure 7C). Moreover, H9-RETR at 10 μg/ml was at least as effective as daclizumab and much more effective than Mikβ1 in inhibiting spontaneous proliferation of cells freshly isolated from a patient with smoldering ATL (Figure 7D), underscoring its potential utility in the control of these vigorously proliferating malignant cells.

DISCUSSION

Partial agonism, defined as reduced signaling amplitude (E_{max}) at ligand saturation, is a pharmacological property typically associated with small molecules targeting G protein-coupled receptors (Strange, 2008), but to a lesser degree for type I transmembrane receptors that signal as dimers (Levin et al., 2014; Riese, 2011). A technical limitation to achieving partial agonism of a dimeric receptor is that, in most cases, wild-type dimerizing ligands (e.g., cytokines, growth factors, etc.) have relatively low

affinity for individual receptor subunits as compared to the dimer and are therefore inefficient clamps. Thus, a dimerizing ligand engineered for high affinity to one of the receptor subunits enables the cytokine to efficiently act as a dominant-negative signal modulator, as has been seen in the interferon system (Levin et al., 2014). Here, we engineered IL-2 variants by enhancing affinity at one receptor binding site (IL-2Rβ) while attenuating interactions at the second receptor binding site (γ_c) in order to manipulate dimerization and signal initiation. Because of augmented binding to IL-2Rβ, these molecules were dominant over endogenous IL-2, and their degree of interaction with γ_c set the intensity of the signal appreciated by the cell, thereby "clamping" signaling amplitude at the partial agonist's E_{max}. Using these partial agonists, we demonstrated that freshly isolated $CD8^+$ T cells and $CD8^+$ T cells pre-activated with anti-CD3 + anti-CD28 had distinct activation thresholds for IL-2 signaling strength, as evidenced by differential effects of H9-T and H9-RET on these cells, whereas H9-RETR, which is an extremely weak partial agonist as shown by its low pSTAT5 induction, had marked inhibitory properties, with potential as an immunosuppressive agent. In particular, it blocked IL-2Rα induction, prolonged survival in a GVHD model, and potently inhibited the spontaneous proliferation of peripheral blood T cells from a patient with smoldering ATL. Moreover, H9-RETR inhibited NK-mediated cytotoxicity.

The effectiveness of anti-CD25 (anti-IL-2Rα) monoclonal antibodies that disrupt high-affinity IL-2 receptor-mediated signaling has stimulated considerable interest in the potential to regulate IL-2 activity as a means of controlling autoimmune diseases and organ rejection. H9-RETR, which is specific for IL-2Rβ but independent of IL-2Rα, might offer therapeutic utility, potentially even in combination with anti-CD25-based therapy. Like H9-RETR, H9-RET almost completely blocked Treg cell differentiation, but unlike H9-RETR, H9-RET could induce proliferation of $CD8^+$ T cells pre-activated with anti-CD3 + anti-CD28. Moreover, H9-T more potently activated STAT5 phosphorylation on activated T cells than on naive cells. These types of partial agonists, unlike full agonists or complete antagonists, might offer the ability to tune the signaling properties to an amplitude that elicits desired functional properties while not meeting thresholds for undesired properties. Given the differential activities of the partial agonists, a larger repertoire of IL-2 variants could be engineered to exhibit an even finer degree of distinctive signaling activities, ranging from almost full to partial agonism to complete antagonism. These could be valuable in dissecting the pleiotropic functions of this cytokine on different immune pathways and might have distinctive therapeutic benefits depending on the context. Indeed, therapeutic agonism by IL-2 might not require the full agonist signal, and benefit might be achieved by delivering a reduced signal amplitude that could mitigate toxicity. Moreover, the rational design approach we have used can be adapted to other γ_c family cytokines and indeed for a broader range of cytokines and growth factors as well.

EXPERIMENTAL PROCEDURES

Protein Expression and Purification

Human IL-2 (amino acids 1–133) and variants thereof, the human IL-2Rβ ectodomain (amino acids 1–214), and the γ_c ectodomain (amino acids 34–232), were secreted and purified via a baculovirus expression system, as previously described (Wang et al., 2005). In brief, all construct sequences were cloned into the pAcGP67A vector (BD Biosciences) with an N-terminal gp67 signal peptide and a C-terminal hexahistidine tag. *Spodoptera frugiperda* (Sf9) insect cells cultured at 28°C in SF900 II SFM medium (Invitrogen) were transfected with the plasmid constructs to establish high-titer recombinant virus, which was subsequently amplified. *Trichopulsia ni* (High-Five) insect cells (Invitrogen) grown in Insect Xpress medium (Lonza) at 28°C were infected with the viruses to express recombinant protein (Kuziel et al., 1993; Yodoi et al., 1985). Three days after infection, proteins were extracted via Ni-NTA (QIAGEN) affinity chromatography, concentrated, and purified to >98% homogeneity with a Superdex 200 sizing column (GE Healthcare) equilibrated in 10 mM HEPES (pH 7.3) and 150 mM NaCl. Fc4 and H9-RETR-Fc4 fusion proteins were also secreted and purified with this system by cloning the human IgG4 Fc domain (Fc4) or the human IL-2 RETR variant followed by a C-terminal human IgG4 Fc domain (H9-RETR-Fc4) into pAcGP67A vector containing an N-terminal gp67 signal peptide and a C-terminal hexahistidine tag. Human IgG4 Fc domain was obtained from a modified pFUSE-hIgG4-Fc vector (Invivogen) with an engineered Ser228 Pro mutation (van der Neut Kolfschoten et al., 2007). For in vivo experiments, endotoxin was removed with Triton X-114 as previously described (Reichelt et al., 2006) and verified with the LAL Chromogenic Endotoxin Quantitation Kit (Thermo Scientific).

For biotinylated protein expression, γ_c with a C-terminal biotin acceptor peptide (BAP)-LNDIFEAQKIEWHE was expressed and purified via Ni-NTA affinity chromatography and biotinylated with soluble BirA ligase enzyme in 0.5 mM Bicine (pH 8.3), 100 mM ATP, 100 mM magnesium acetate, and 500 mM biotin (Sigma). Proteins were purified by size exclusion on a Superdex 200 column as above.

Surface Plasmon Resonance Binding Measurements

Binding interactions were characterized via surface plasmon resonance (SPR) with Biacore SA sensor chips (GE Healthcare) on a Biacore T100 instrument. γ_c was immobilized to the chip surface at low density (RU_{max} < 100 response units), and serial dilutions of H9:IL-2Rβ or H9-RET:IL-2Rβ complexes were exposed to the surface for 60 s. Dissociation was then tracked for 200 s. An irrelevant biotinylated protein was immobilized in the reference channel to subtract non-specific binding. Experiments were performed in HBS-P+ buffer (GE Healthcare) supplemented with 0.2% BSA at 25°C at a flow rate of 30 ml/min to minimize mass transport contributions and prevent rebinding of the analyte. Data analysis and determination of equilibrium and kinetic parameters were implemented with the Biacore T100 evaluation software v.2.0 assuming a 1:1 Langmuir binding model.

Tissue Culture and Magnetic Purification of $CD25^+$ YT-1 Cells

Unmodified YT (Yodoi et al., 1985) and $CD25^+$ YT-1 (Kuziel et al., 1993) natural killer-like cells were cultured in RPMI complete medium (RPMI 1640 medium with 10% fetal bovine serum, 2 mM L-glutamine, minimum non-essential amino acids, sodium pyruvate, 25 mM HEPES, and penicillin-streptomycin [GIBCO]) at 37°C in a humidified atmosphere with 5% CO_2.

Subpopulations of YT-1 cells expressing or not expressing CD25 were purified via magnetic selection, as described (Ring et al., 2012). Ten million unsorted $CD25^+$ YT-1 cells were washed with flow cytometry buffer (phosphate-buffered saline [pH 7.2] containing 0.1% bovine serum albumin) and incubated with PE-conjugated anti-human CD25 antibody (Biolegend, clone BC96) in flow cytometry buffer for 2 hr at 4°C. The PE-stained $CD25^+$ cells were labeled with paramagnetic microbeads conjugated to an anti-PE IgG for 20 min at 4°C, washed once with cold flow cytometry buffer, and sorted with an LS MACS separation column (Miltenyi Biotec) according to the manufacturer's protocol. Eluted cells were re-suspended and grown in RPMI complete medium and enrichment of $CD25^+$ cells was evaluated with an Accuri C6 flow cytometer. Persistence of CD25 expression on the sorted $CD25^+$ YT-1 cells was monitored by flow cytometric analysis with PE-conjugated anti-human CD25 antibody. Detailed methods for phosphor-flow analysis is described in the Supplemental Experimental Procedures.

IL-2 Receptor Internalization Experiments

IL-2, H9, H9-RET, or H9 RETR (1 μM) was incubated with 3 × 10^5 YT-1 cells in a 96-well plate for 2, 5, 10, 15, 30, 60, 90, 120, 180, or 240 min. Cells were immediately transferred to ice to prevent further receptor internalization and washed twice with ice-cold PBSA buffer (0.1% BSA in PBS) and stained with 1:50 dilutions of allophycocyanin-conjugated anti-human IL-2Rβ antibody (TU27; Biolegend) and phycoerythrin-conjugated anti-human IL-2Rγ antibody (TUGh4; Biolegend) in PBSA buffer for 30 min on ice. After two more washes in ice-cold PBSA buffer, cells were fixed for 10 min at room temperature with 1.5% paraformaldehyde in PBSA, washed, and resuspended in PBSA buffer. Mean cell fluorescence was quantified with an Accuri C6 flow cytometer. Internalization data were fitted to a single exponential decay model via non-linear least-squares regression with the Prism software package (GraphPad).

Human $CD8^+$ T Cell Isolation and Intracellular Staining of pSTAT5 and pS6-Ribosomal Protein

Buffy coats were from healthy donors from the NIH Blood Bank. Peripheral blood mononuclear cells (PBMCs) were isolated by gradient centrifugation using lymphocyte separation medium (Mediatech). Cells were isolated with the human $CD8^+$ T cell isolation kit I (Miltenyi Biotec). To pre-activate cells, 6-well plates were pre-coated with 2 μg/ml of plate-bound anti-CD3 mAb (BD Biosciences), cells were seeded at 1 × 10^6 cells/ml in complete medium (RPMI medium supplemented with glutamine, penicillin, streptomycin, and 10% FBS) with 1 μg/ml soluble anti-CD28 mAb (BD Biosciences) for 3 days and then rested for 48 hr in fresh medium. The methods for phospho-flow cytometry, thymidine incorporation, immunoblotting, CFSE dilution, and EdU proliferation assays are described in the Supplemental Experimental Procedures.

Analysis of STAT5 Phosphorylation Ex Vivo

C57BL/6 mice were from the Jackson Laboratory. Animal protocols were approved by the NHLBI Animal Care and Use Committee and followed the NIH Guidelines, "Using Animals in Intramural Research." STAT5 phosphorylation was assayed by the manufacturer's protocol (BD Bioscience). In brief, H9-RETR-Fc4 fusion protein or Fc4 control or anti-mouse IL-2Rα monoclonal Ab PC61 (BioXcell) or rat IgG1 isotype control were injected i.p. into C57BL/6 mice 1 hr prior to IL-2 or IL-15 injection, and total splenocytes isolated, immediately fixed with BD Phosphoflow Lyse/Fix buffer, washed twice with ice-cold PBS, stained with anti-CD4 (Biolegend), and permeabilized with BD PhosFlow Perm Buffer III for 30 min on ice in the dark. Cells were then washed twice with ice-cold flow cytometry buffer, stained with anti-FoxP3 per the manufacturer's protocol (eBioscience), washed twice with ice-cold flow cytometry buffer, and stained with anti-phospho-STAT5-PE (1:30) (BD) at room temperature for 30 min in the dark. Cells were washed three times with flow cytometry buffer and data acquired on a BD FACSCanto II flow cytometer and analyzed with FlowJo (Tree Star). We used human IL-2 for these mouse studies as is typical (Rosenberg et al., 1985; Tang et al., 2008) given the proven efficacy of human IL-2 in the mouse.

Proliferation of ED40515 Cells and Cells from a Patient with Smoldering ATL

IL-2-dependent ED40515(+) (Maeda et al., 1985) cells were washed twice with PBS. Cells were seeded into 96-well plates at 1 × 10^4 cells/well in 100 μl of RPMI 1640 medium with or without IL-2 and with or without reagents and then incubated at 37°C for 3 days.

Blood samples from ATL patients were obtained under the care of the Clinical Trials Team, Lymphoid Malignancies Branch, NCI, NIH. This study protocol was approved by the Institutional Review Board of the National Cancer Institute. Informed consent was obtained in accordance with the Declaration of Helsinki. Peripheral blood mononuclear cells (PBMCs) from ATL patients were isolated by Ficoll-Hypaque density gradient centrifugation from heparinized blood. Aliquots of 1 × 10^5 cells/100 μl/well were cultured ex vivo in RPMI 1640 medium supplemented with 10% FBS with or without reagents for 6 days. During the last 6 hr of culture, ED40515(+) cells or ATL PBMCs were pulsed with 1 μCi (0.037 MBq) [^{3}H]thymidine, and cells were then harvested (Tomtec) and counted with a MicroBeta2 microplate counter (PerkEmer). The assay was performed in triplicate.

Activation of NK Cells and NK Cell Cytotoxicity Assay

Peripheral blood mononuclear cells (PBMCs) were cultured in the presence of 1 μg/ml IL-2 analogs for 24 hr. Cells were then stained with APC-conjugated anti-CD56 (BD Biosciences), Pacific Blue-conjugated anti-CD3 (BioLegend), and FITC-conjugated anti-CD69 (BD Biosciences). Samples were analyzed by flow cytometry with a FACSAria II (BD Biosciences). NK cells were gated as CD3-negative, CD56-positive.

PBMCs were isolated by gradient centrifugation with Ficoll-Paque Premium (GE Life Sciences), and then untouched NK cells were purified with the Human NK Cell Isolation Kit (Miltenyi) followed by separation with an autoMACS (Miltenyi). HER18 target cells were labeled with 150 μCi ^{51}Cr (Perkin Elmer) per 1 × 10^6 cells for 2 hr. NK cells were added to 10,000 HER18 cells at a 10:1 effector:target ratio. Specific lysis was determined after 4 hr of culture in the presence of varying concentrations of IL-2 variants.

Lysis of K562 cells by primary NK cells was performed as described (Thomas et al., 2013). In brief, human NK cells were purified with a kit (STEMCELL). K562 cells were labeled with the PKH67 green fluorescent cell linker kit (Sigma-Aldrich) and NK cells were added to 5,000 K562 cells at a 10:1 ratio, cultured in the presence of varying concentrations of IL-2 variants at 37°C for 4 hr, and placed on ice to prevent further reactivity. Cells were then stained with propidium iodide (PI) (Sigma-Aldrich) and the percentage of PI^+ $PKH67^+$ K562 cells was determined by flow cytometry.

T Helper Cell Polarization and Intracellular Cytokine Staining

Naive $CD4^+$ C57BL/6 T cells were differentiated under different T helper cell polarization conditions in the absence or presence of the indicated cytokines. Four days later, cells were first stained for surface antigens as indicated and then with antibodies to IFN-γ (eBioscience), IL-17A (eBioscience), IL-4 (BioLegend), IL-9 (BioLegend), or FoxP3 (eBioscience) in BD cytofix and cytoperm or via the eBioscience FoxP3 staining buffer kit according to the manufacturer's protocol. Stained cells were analyzed on a FACSCanto II flow cytometer (Becton Dickinson) with FlowJo software (Tree Star). All mouse cytokines were from Peprotech.

RNA-Seq Analysis

$CD8^+$ T cells were pre-activated with anti-CD3 + anti-CD28, rested for 2 days in complete medium, and stimulated for 24 hr with 1 μg/ml of wild-type IL-2, H9, H9-RET, or H9-RETR, and total RNA from 5 × 10^6 cells was isolated (RNeasy kit, QIAGEN). RNA from five donors was pooled, and 1 μg of the pooled RNA was used to synthesize cDNA. RNA-seq libraries were prepared as described (Ring et al., 2012). PCR-amplified products were barcoded and sequenced with an Illumina HiSeq2000 platform. Sequenced reads were aligned against the human genome (hg18, NCBI build 36.1) with Bowtie 0.12.4 (Langmead et al., 2009). Uniquely mapped reads were retained, and digital expression of genes was calculated with RPKM (Reads Per Kilobase per Million mapped reads). R package edgeR was used to identify differentially expressed genes, and fold-change (in log2 scale) differences were compared between cells not treated or treated with the IL-2 variants for 24 hr.

ChIP-Seq Library Preparation and Analysis

$CD8^+$ T cells were pre-activated with anti-CD3 + anti-CD28, treated with different cytokines for 90 min, and then chemically cross-linked with 1% paraformaldehyde. Chromatin from 10–20 million cells was sonicated into 250–500 bp fragments, immunoprecipitated with anti-STAT5B (Invitrogen), and processed for sequencing as described (Liao et al., 2008). All reads were aligned against the human genome (hg18, NCBI build 36.1) with Bowtie 0.12.4. Uniquely mapped reads were converted to browser extensible data (BED) files and duplicated reads (multiple reads in same genomic location) were filtered. The filtered (non-redundant) BED files were then converted to binary tiled data (.tdf) and visualized with the Integrative Genome Viewer (Broad Institute).

Gene Expression Analysis by RT-PCR

Total RNA was isolated with RNeasy Plus mini kit (QIAGEN) and 200 ng was used together with oligo dT (Invitrogen) and the Omniscript reverse transcription kit (Quiagen) to synthesize cDNA. Quantitative RT-PCR was performed

with an ABI 7900 HD Sequence Detection System. RT primers and probes were from Applied Biosystems. Expression was normalized to *RPL7*.

Bone Marrow Transplantation into Allogeneic Hosts

7-week-old female C57BL/6 (H_2K^b) and BALB/c (H_2K^d) mice from the NCI-Frederick Cancer Research Facility were maintained in a specific-pathogen-free facility and treated according to an animal protocol approved by the NCI Animal Care and Use Committee. BALB/c mice were conditioned with 950 cGy total body irradiation and then reconstituted with 10 million T-cell-depleted bone marrow cells from C57BL/6 mice alone or together with 2 million Treg-cell-depleted pan-T cells. T cell depletion was performed with anti-CD90 (Thy1.2) microbeads (total T cell depletion) or anti-CD25 (Treg cell depletion) with kits from Miltenyi Biotec. Mice receiving pan-T cells were additionally treated with Fc4 or H9-RETR-Fc4 (100 μg i.p. twice/day for 10 days). Drinking water was supplemented with ciprofloxacin from day −1 to +14 after total body irradiation. Survival was monitored. Survival was analyzed according to the Kaplan-Meier method, and survival curves were compared via the log-rank test. Statistical analysis was performed with GraphPad Prism 4 software.

ACCESSION NUMBERS

The ChIP-seq and RNA-seq data reported in this paper and tabulated in part in Table S1 are accessible through GEO SuperSeries accession number GEO: GSE64713.

SUPPLEMENTAL INFORMATION

Supplemental Information includes three figures, one table, and Supplemental Experimental Procedures and can be found with this article online at http://dx.doi.org/10.1016/j.immuni.2015.04.018.

AUTHOR CONTRIBUTIONS

S.M., A.M.R., K.C.G., and W.J.L. conceived of most of the study. S.M. and A.M.R. performed most of the experiments. S.A., J.B.S., W.J., S.F., J.O., R.S., K.W., H.K., J.E.F., and S.R. performed or contributed to specific experiments. P.L. performed the bioinformatics analysis. D.H.F., E.O.L., and T.A.W. provided support and direction for specific experiments and valuable discussions. All authors helped to design experiments and/or analyze data. S.M., A.M.R., K.C.G., and W.J.L. wrote the manuscript, with contribution from all of the authors.

ACKNOWLEDGMENTS

This work was supported by the Divisions of Intramural Research, National Heart, Lung, and Blood Institute (S.M., P.L., J.O., R.S., and W.J.L.), National Cancer Institute (S.M., W.J., D.H.F., and T.A.W.), National Institute of Allergy and Infectious Diseases (S.R. and E.O.L), NIH-R0AI51321 (K.C.G.), and NIH-F30DK094541 (A.M.R.). K.C.G. is an investigator of the Howard Hughes Medical Institute. J.B.S. is the recipient of a Leukemia & Lymphoma Society Career Development Program fellowship. We thank Dr. Junji Yodoi, Kyoto University, for YT and YT-1 NK-like cells.

Received: February 4, 2015
Revised: April 9, 2015
Accepted: April 29, 2015
Published: May 19, 2015

REFERENCES

Beniaminovitz, A., Itescu, S., Lietz, K., Donovan, M., Burke, E.M., Groff, B.D., Edwards, N., and Mancini, D.M. (2000). Prevention of rejection in cardiac transplantation by blockade of the interleukin-2 receptor with a monoclonal antibody. N. Engl. J. Med. *342*, 613–619.

Bielekova, B., Richert, N., Howard, T., Blevins, G., Markovic-Plese, S., McCartin, J., Frank, J.A., Würfel, J., Ohayon, J., Waldmann, T.A., et al. (2004). Humanized anti-CD25 (daclizumab) inhibits disease activity in multiple sclerosis patients failing to respond to interferon beta. Proc. Natl. Acad. Sci. USA *101*, 8705–8708.

Blaser, B.W., Roychowdhury, S., Kim, D.J., Schwind, N.R., Bhatt, D., Yuan, W., Kusewitt, D.F., Ferketich, A.K., Caligiuri, M.A., and Guimond, M. (2005). Donor-derived IL-15 is critical for acute allogeneic graft-versus-host disease. Blood *105*, 894–901.

Boyman, O., and Sprent, J. (2012). The role of interleukin-2 during homeostasis and activation of the immune system. Nat. Rev. Immunol. *12*, 180–190.

Cheng, G., Yu, A., and Malek, T.R. (2011). T-cell tolerance and the multi-functional role of IL-2R signaling in T-regulatory cells. Immunol. Rev. *241*, 63–76.

Chinen, J., and Buckley, R.H. (2010). Transplantation immunology: solid organ and bone marrow. J. Allergy Clin. Immunol. *125* (2), S324–S335.

Donohue, J.H., and Rosenberg, S.A. (1983). The fate of interleukin-2 after in vivo administration. J. Immunol. *130*, 2203–2208.

Ferrara, J.L., Marion, A., McIntyre, J.F., Murphy, G.F., and Burakoff, S.J. (1986). Amelioration of acute graft vs host disease due to minor histocompatibility antigens by in vivo administration of anti-interleukin 2 receptor antibody. J. Immunol. *137*, 1874–1877.

Gold, R., Giovannoni, G., Selmaj, K., Havrdova, E., Montalban, X., Radue, E.W., Stefoski, D., Robinson, R., Riester, K., Rana, J., et al.; SELECT study investigators (2013). Daclizumab high-yield process in relapsing-remitting multiple sclerosis (SELECT): a randomised, double-blind, placebo-controlled trial. Lancet *381*, 2167–2175.

Hémar, A., Subtil, A., Lieb, M., Morelon, E., Hellio, R., and Dautry-Varsat, A. (1995). Endocytosis of interleukin 2 receptors in human T lymphocytes: distinct intracellular localization and fate of the receptor alpha, beta, and gamma chains. J. Cell Biol. *129*, 55–64.

Hershberger, R.E., Starling, R.C., Eisen, H.J., Bergh, C.H., Kormos, R.L., Love, R.B., Van Bakel, A., Gordon, R.D., Popat, R., Cockey, L., and Mamelok, R.D. (2005). Daclizumab to prevent rejection after cardiac transplantation. N. Engl. J. Med. *352*, 2705–2713.

Ju, W., Zhang, M., Jiang, J.K., Thomas, C.J., Oh, U., Bryant, B.R., Chen, J., Sato, N., Tagaya, Y., Morris, J.C., et al. (2011). CP-690,550, a therapeutic agent, inhibits cytokine-mediated Jak3 activation and proliferation of T cells from patients with ATL and HAM/TSP. Blood *117*, 1938–1946.

Kalia, V., Sarkar, S., Subramaniam, S., Haining, W.N., Smith, K.A., and Ahmed, R. (2010). Prolonged interleukin-2Ralpha expression on virus-specific CD8+ T cells favors terminal-effector differentiation in vivo. Immunity *32*, 91–103.

Kim, H.P., Imbert, J., and Leonard, W.J. (2006). Both integrated and differential regulation of components of the IL-2/IL-2 receptor system. Cytokine Growth Factor Rev. *17*, 349–366.

Kuziel, W.A., Ju, G., Grdina, T.A., and Greene, W.C. (1993). Unexpected effects of the IL-2 receptor alpha subunit on high affinity IL-2 receptor assembly and function detected with a mutant IL-2 analog. J. Immunol. *150*, 3357–3365.

Langmead, B., Trapnell, C., Pop, M., and Salzberg, S.L. (2009). Ultrafast and memory-efficient alignment of short DNA sequences to the human genome. Genome Biol. *10*, R25.

Laurence, A., Tato, C.M., Davidson, T.S., Kanno, Y., Chen, Z., Yao, Z., Blank, R.B., Meylan, F., Siegel, R., Hennighausen, L., et al. (2007). Interleukin-2 signaling via STAT5 constrains T helper 17 cell generation. Immunity *26*, 371–381.

Lenardo, M.J. (1991). Interleukin-2 programs mouse alpha beta T lymphocytes for apoptosis. Nature *353*, 858–861.

Levin, A.M., Bates, D.L., Ring, A.M., Krieg, C., Lin, J.T., Su, L., Moraga, I., Raeber, M.E., Bowman, G.R., Novick, P., et al. (2012). Exploiting a natural conformational switch to engineer an interleukin-2 'superkine'. Nature *484*, 529–533.

Levin, D., Schneider, W.M., Hoffmann, H.H., Yarden, G., Busetto, A.G., Manor, O., Sharma, N., Rice, C.M., and Schreiber, G. (2014). Multifaceted activities of type I interferon are revealed by a receptor antagonist. Sci. Signal. *7*, ra50.

Liao, W., Schones, D.E., Oh, J., Cui, Y., Cui, K., Roh, T.Y., Zhao, K., and Leonard, W.J. (2008). Priming for T helper type 2 differentiation by interleukin

2-mediated induction of interleukin 4 receptor alpha-chain expression. Nat. Immunol. *9*, 1288–1296.

Liao, W., Lin, J.X., Wang, L., Li, P., and Leonard, W.J. (2011). Modulation of cytokine receptors by IL-2 broadly regulates differentiation into helper T cell lineages. Nat. Immunol. *12*, 551–559.

Liao, W., Lin, J.X., and Leonard, W.J. (2013). Interleukin-2 at the crossroads of effector responses, tolerance, and immunotherapy. Immunity *38*, 13–25.

Littman, D.R., and Rudensky, A.Y. (2010). Th17 and regulatory T cells in mediating and restraining inflammation. Cell *140*, 845–858.

Maeda, M., Shimizu, A., Ikuta, K., Okamoto, H., Kashihara, M., Uchiyama, T., Honjo, T., and Yodoi, J. (1985). Origin of human T-lymphotrophic virus I-positive T cell lines in adult T cell leukemia. Analysis of T cell receptor gene rearrangement. J. Exp. Med. *162*, 2169–2174.

Morgan, D.A., Ruscetti, F.W., and Gallo, R. (1976). Selective in vitro growth of T lymphocytes from normal human bone marrows. Science *193*, 1007–1008.

Morris, J.C., Janik, J.E., White, J.D., Fleisher, T.A., Brown, M., Tsudo, M., Goldman, C.K., Bryant, B., Petrus, M., Top, L., et al. (2006). Preclinical and phase I clinical trial of blockade of IL-15 using Mikbeta1 monoclonal antibody in T cell large granular lymphocyte leukemia. Proc. Natl. Acad. Sci. USA *103*, 401–406.

Nakamura, Y., Russell, S.M., Mess, S.A., Friedmann, M., Erdos, M., Francois, C., Jacques, Y., Adelstein, S., and Leonard, W.J. (1994). Heterodimerization of the IL-2 receptor beta- and gamma-chain cytoplasmic domains is required for signalling. Nature *369*, 330–333.

Nelson, B.H., Lord, J.D., and Greenberg, P.D. (1994). Cytoplasmic domains of the interleukin-2 receptor beta and gamma chains mediate the signal for T-cell proliferation. Nature *369*, 333–336.

Noguchi, M., Yi, H., Rosenblatt, H.M., Filipovich, A.H., Adelstein, S., Modi, W.S., McBride, O.W., and Leonard, W.J. (1993). Interleukin-2 receptor gamma chain mutation results in X-linked severe combined immunodeficiency in humans. Cell *73*, 147–157.

Pipkin, M.E., Sacks, J.A., Cruz-Guilloty, F., Lichtenheld, M.G., Bevan, M.J., and Rao, A. (2010). Interleukin-2 and inflammation induce distinct transcriptional programs that promote the differentiation of effector cytolytic T cells. Immunity *32*, 79–90.

Reichelt, P., Schwarz, C., and Donzeau, M. (2006). Single step protocol to purify recombinant proteins with low endotoxin contents. Protein Expr. Purif. *46*, 483–488.

Rickert, M., Wang, X., Boulanger, M.J., Goriatcheva, N., and Garcia, K.C. (2005). The structure of interleukin-2 complexed with its alpha receptor. Science *308*, 1477–1480.

Riese, D.J., 2nd. (2011). Ligand-based receptor tyrosine kinase partial agonists: New paradigm for cancer drug discovery? Expert Opin Drug Discov *6*, 185–193.

Ring, A.M., Lin, J.X., Feng, D., Mitra, S., Rickert, M., Bowman, G.R., Pande, V.S., Li, P., Moraga, I., Spolski, R., et al. (2012). Mechanistic and structural insight into the functional dichotomy between IL-2 and IL-15. Nat. Immunol. *13*, 1187–1195.

Rochman, Y., Spolski, R., and Leonard, W.J. (2009). New insights into the regulation of T cells by gamma(c) family cytokines. Nat. Rev. Immunol. *9*, 480–490.

Rosenberg, S.A. (2014). IL-2: the first effective immunotherapy for human cancer. J. Immunol. *192*, 5451–5458.

Rosenberg, S.A., Mulé, J.J., Spiess, P.J., Reichert, C.M., and Schwarz, S.L. (1985). Regression of established pulmonary metastases and subcutaneous tumor mediated by the systemic administration of high-dose recombinant interleukin 2. J. Exp. Med. *161*, 1169–1188.

Strange, P.G. (2008). Agonist binding, agonist affinity and agonist efficacy at G protein-coupled receptors. Br. J. Pharmacol. *153*, 1353–1363.

Strohl, W.R. (2009). Optimization of Fc-mediated effector functions of monoclonal antibodies. Curr. Opin. Biotechnol. *20*, 685–691.

Tang, Q., Adams, J.Y., Penaranda, C., Melli, K., Piaggio, E., Sgouroudis, E., Piccirillo, C.A., Salomon, B.L., and Bluestone, J.A. (2008). Central role of defective interleukin-2 production in the triggering of islet autoimmune destruction. Immunity *28*, 687–697.

Thomas, L.M., Peterson, M.E., and Long, E.O. (2013). Cutting edge: NK cell licensing modulates adhesion to target cells. J. Immunol. *191*, 3981–3985.

van der Neut Kolfschoten, M., Schuurman, J., Losen, M., Bleeker, W.K., Martínez-Martínez, P., Vermeulen, E., den Bleker, T.H., Wiegman, L., Vink, T., Aarden, L.A., et al. (2007). Anti-inflammatory activity of human IgG4 antibodies by dynamic Fab arm exchange. Science *317*, 1554–1557.

Vincenti, F., Kirkman, R., Light, S., Bumgardner, G., Pescovitz, M., Halloran, P., Neylan, J., Wilkinson, A., Ekberg, H., Gaston, R., et al.; Daclizumab Triple Therapy Study Group (1998). Interleukin-2-receptor blockade with daclizumab to prevent acute rejection in renal transplantation. N. Engl. J. Med. *338*, 161–165.

Waldmann, T.A. (2006). The biology of interleukin-2 and interleukin-15: implications for cancer therapy and vaccine design. Nat. Rev. Immunol. *6*, 595–601.

Waldmann, T.A., Conlon, K.C., Stewart, D.M., Worthy, T.A., Janik, J.E., Fleisher, T.A., Albert, P.S., Figg, W.D., Spencer, S.D., Raffeld, M., et al. (2013). Phase 1 trial of IL-15 trans presentation blockade using humanized Mikβ1 mAb in patients with T-cell large granular lymphocytic leukemia. Blood *121*, 476–484.

Wang, X., Rickert, M., and Garcia, K.C. (2005). Structure of the quaternary complex of interleukin-2 with its alpha, beta, and gammac receptors. Science *310*, 1159–1163.

Yodoi, J., Teshigawara, K., Nikaido, T., Fukui, K., Noma, T., Honjo, T., Takigawa, M., Sasaki, M., Minato, N., Tsudo, M., et al. (1985). TCGF (IL 2)-receptor inducing factor(s). I. Regulation of IL 2 receptor on a natural killer-like cell line (YT cells). J. Immunol. *134*, 1623–1630.

Yu, A., Zhu, L., Altman, N.H., and Malek, T.R. (2009). A low interleukin-2 receptor signaling threshold supports the development and homeostasis of T regulatory cells. Immunity *30*, 204–217.

Zhu, J., Yamane, H., and Paul, W.E. (2010). Differentiation of effector CD4 T cell populations (*). Annu. Rev. Immunol. *28*, 445–489.

Zurawski, S.M., Vega, F., Jr., Doyle, E.L., Huyghe, B., Flaherty, K., McKay, D.B., and Zurawski, G. (1993). Definition and spatial location of mouse interleukin-2 residues that interact with its heterotrimeric receptor. EMBO J. *12*, 5113–5119.

Immunity

Supplemental Information

Interleukin-2 Activity Can Be Fine Tuned with Engineered Receptor Signaling Clamps

Suman Mitra, Aaron M. Ring, Shoba Amarnath, Jamie B. Spangler, Peng Li, Wei Ju, Suzanne Fischer, Jangsuk Oh, Rosanne Spolski, Kipp Weiskopf, Holbrook Kohrt, Jason E. Foley, Sumati Rajagopalan, Eric O. Long, Daniel H. Fowler, Thomas A. Waldmann, K. Christopher Garcia, and Warren J. Leonard

Table S1, related to Figure 4. Genes that are up- or down-regulated by IL-2, H9, H9-RET, and H9-RETR as compared to unstimulated control cells. Note that this is provided as a separate Excel file.

Figure S1, related to Figure 2. Effects of IL-2 variants on pERK. (A and **B)** Dose-response curves of phospho-ERK1/ERK2 protein on $CD25^+$ (**A**) and $CD25^-$ (**B**) YT1 human NK-like cells. **(C)** Comparison of IL-2Rβ and IL-2Rγ expression on freshly isolated (upper panels) or pre-activated (lower panels) human $CD8^+$ T cells. Data are representative of at least two experiments per panel. Error bars in **(A)** represent S.E.M. of triplicates.

Figure S2, related to Figure 5. Effect of H9-RET and H9-RETR on CD25 expression, IL-2- and IL-15-induced proliferation, and TCR-induced proliferation of $CD8^+$ T cells, and the differentiation of Th1, Th17, Th9, and iTreg cells.
(A) H9-RET and H9-RETR inhibited IL-2-induced CD25 expression on pre-activated $CD8^+$ T cells. The numbers represent the percentage of cells in the corresponding quadrants. Data are representative of three independent experiments.
(B) Inhibition of IL-2- and IL-15-induced proliferation by H9-RET and H9-RETR. Freshly isolated $CD8^+$ T cell were CFSE-labeled and stimulated with IL-2 or IL-15 (1 μg/ml) in the presence or absence of 1 μg/ml H9-RET or H9-RETR, and CFSE dilution assessed. Data are representative of three independent experiments.
(C) Both H9-RET and H9-RETR inhibit TCR-induced proliferation of freshly isolated $CD8^+$ T cells. Cells were labeled with CFSE, stimulated with plate bound anti-CD3 (2

μg/ml) + soluble anti-CD28 (1 μg/ml) for 4 days with or without 1 μg/ml of H9-RET or H9-RETR, and CFSE dilution assessed by flow cytometry.

(D) 1 μg/ml of either H9-RET or H9-RETR inhibited TCR-induced CD25 expression on peripheral blood $CD8^+$ T cells stimulated for 4 days with 2 μg/ml anti-CD3 + 1 μg/ml anti-CD28. Data are representative of three independent experiments.

(**E**) H9-RET and H9-RETR block Th1, Th9, and Treg differentiation but promote Th17 differentiation. Cells were differentiated under various T-helper polarizing conditions in the absence or presence of H9-RET or H9-RETR. Data are representative of at least two independent experiments for each type of cell.

Figure S3, related to Figure 6. Relative potency *in vivo* of H9-RETR-Fc4 versus an anti-mouse-IL-2Rα blocking antibody (clone PC61).

H9-RETR-Fc4 was more effective in blocking IL-2-induced pSTAT5 signaling than PC61 *in vivo*. Left, C57BL/6 mice were injected i.p. with PBS or 1 μg IL-2. Right, C57BL/6 mice were injected with 100 μg of control rat IgG1, PC61, or H9-RETR-Fc4 60 min prior to injection of 1 μg IL-2. pSTAT5 was measured 30 min later in splenic $CD4^+CD25^+FoxP3^+$ T cells. MFIs are indicated. Data are representative of two independent experiments.

Figure S1

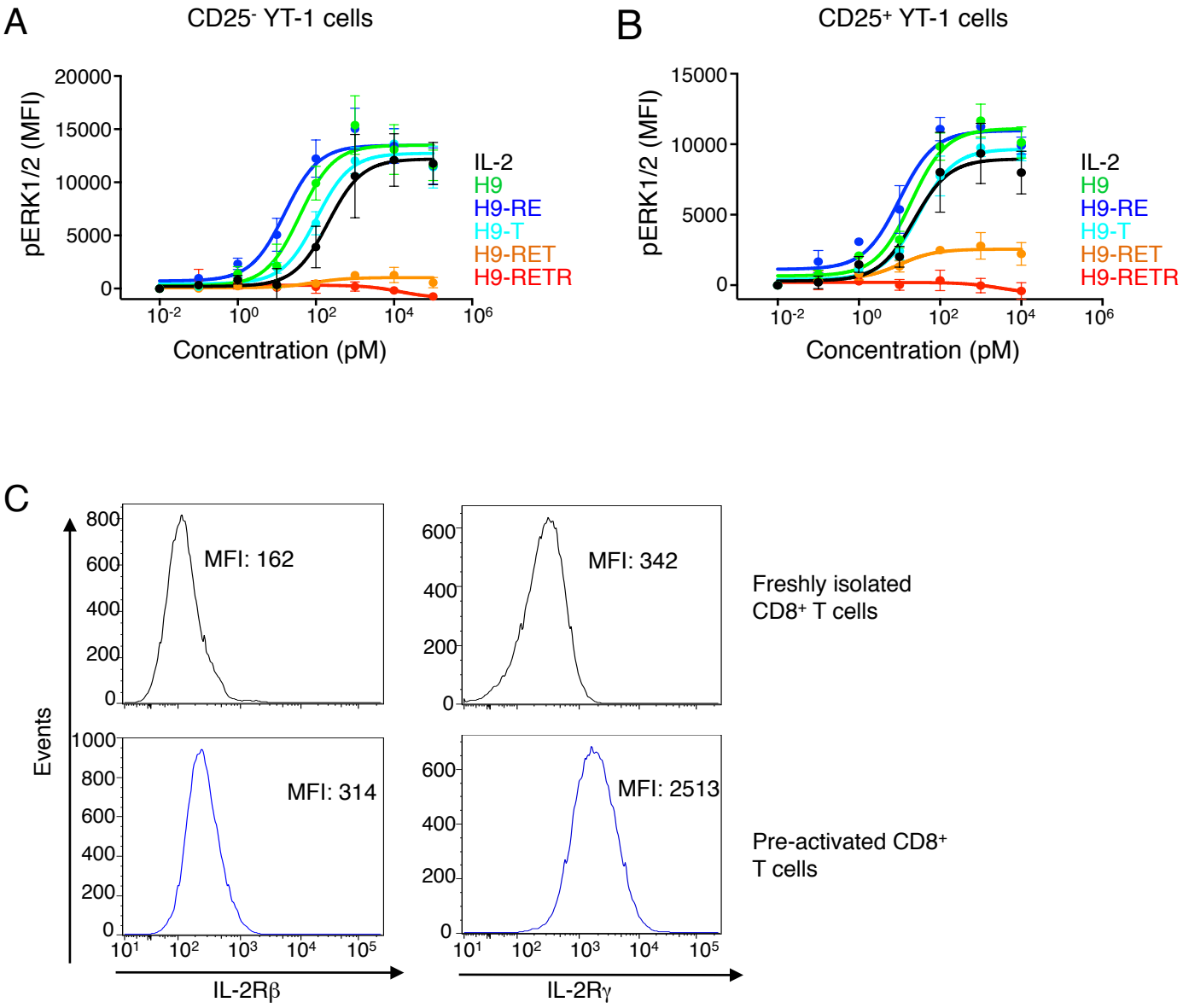
A
CD25- YT-1 cells
pERK1/2 (MFI)
20000
15000
10000
5000
0
10-2
100
102
104
106
Concentration (pM)
IL-2
H9
H9-RE
H9-T
H9-RET
H9-RETR
B
CD25+ YT-1 cells
pERK1/2 (MFI)
15000
10000
5000
0
10-2
100
102
104
106
Concentration (pM)
IL-2
H9
H9-RE
H9-T
H9-RET
H9-RETR
C
Events
MFI: 162
MFI: 342
MFI: 314
MFI: 2513
IL-2Rβ
IL-2Rγ
Freshly isolated
CD8+ T cells
Pre-activated CD8+
T cells

Figure S2

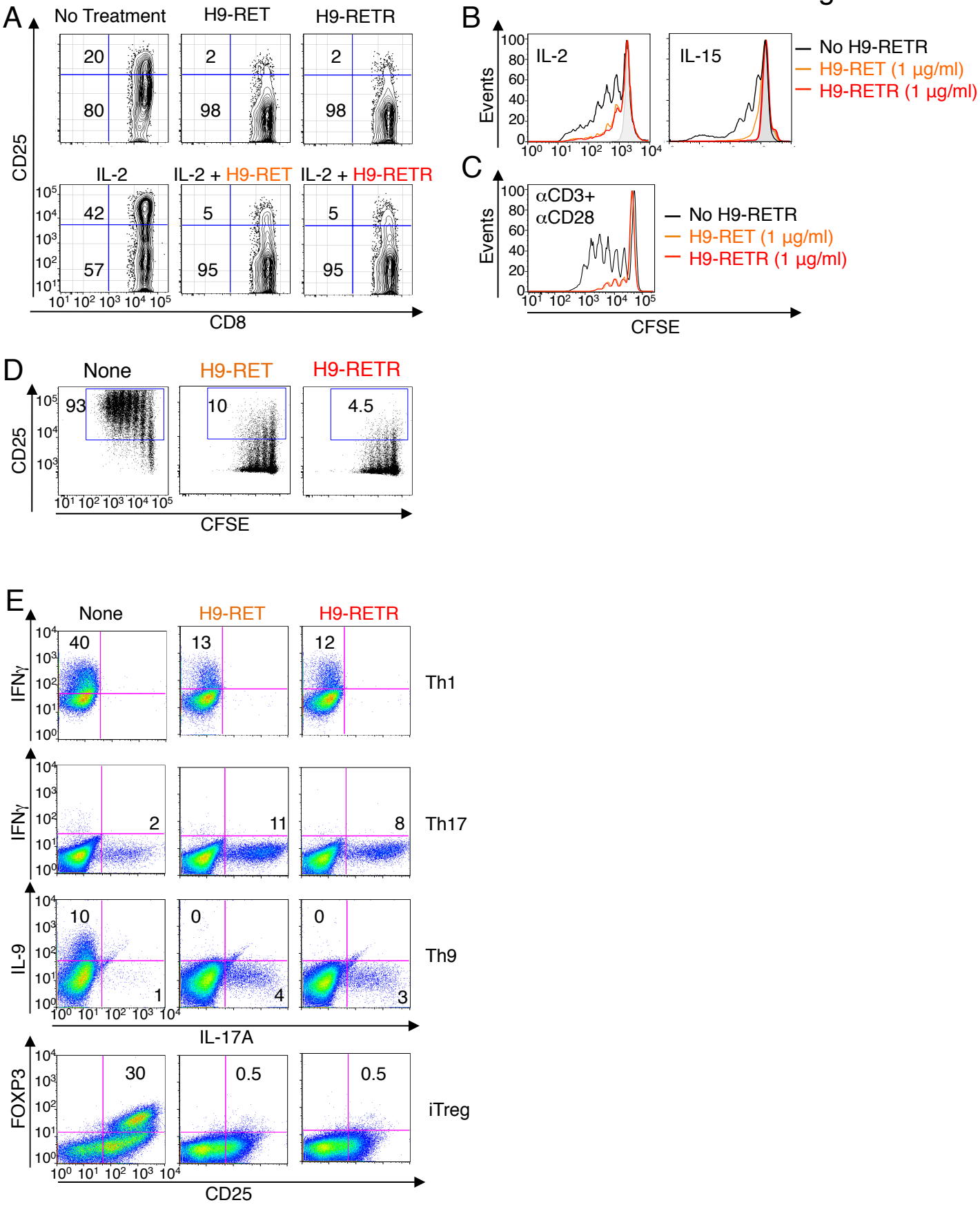
A
No Treatment
H9-RET
H9-RETR
20
80
2
98
2
98
IL-2
IL-2 + H9-RET
IL-2 + H9-RETR
42
57
5
95
5
95
CD25
CD8
B
IL-2
IL-15
Events
No H9-RETR
H9-RET (1 µg/ml)
H9-RETR (1 µg/ml)
C
αCD3+
αCD28
Events
No H9-RETR
H9-RET (1 µg/ml)
H9-RETR (1 µg/ml)
CFSE
D
None
H9-RET
H9-RETR
93
10
4.5
CD25
CFSE
E
None
H9-RET
H9-RETR
40
13
12
Th1
IFNγ
2
11
8
Th17
IFNγ
10
1
0
4
0
3
Th9
IL-9
IL-17A
30
0.5
0.5
iTreg
FOXP3
CD25

Figure S3

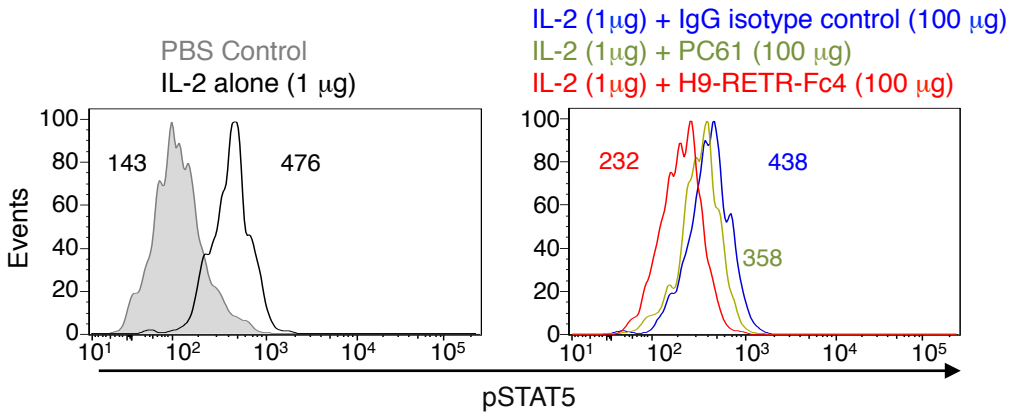
PBS Control
IL-2 alone (1 μg)
IL-2 (1μg) + IgG isotype control (100 μg)
IL-2 (1μg) + PC61 (100 μg)
IL-2 (1μg) + H9-RETR-Fc4 (100 μg)
Events
143
476
232
438
358
pSTAT5

Supplemental Experimental Procedures

Flow Cytometric Analysis of Intracellular Phospho-STAT5 and Phospho-ERK1-ERK2 Approximately 2 x 10^5 YT or $CD25^+$ YT-1 cells were plated in wells of a 96-well plate, washed with flow cytometry buffer, and re-suspended in flow cytometry buffer containing serial dilutions of IL-2, H9, H9-RET, or H9-RETR. Cells were stimulated for 20 min at 37ºC, fixed by addition of formaldehyde to 1.5%, incubated for 10 min at room temperature, and permeabilized with 100% ice-cold methanol for 30 min at 4ºC to allow for detection of intracellular signal effectors. The fixed and permeabilized cells were washed twice with flow cytometry buffer and incubated with Alexa488-conjugated anti-STAT5 pY694 (BD Biosciences) or Alexa488-conjugated anti-ERK1-ERK2 pT202/pY204 (BD Biosciences) diluted in flow cytometry buffer for 2 hr at room temperature. Cells were then washed twice in flow cytometry buffer and mean fluorescence intensity (MFI) was quantified on an Accuri C6 flow cytometer (BD Biosciences). Dose-response curves were generated, and EC_{50} and E_{max} values were calculated using the GraphPad Prism data analysis software after subtracting the MFI of unstimulated cells and normalizing to the maximum signal intensity induced by cytokine stimulation.

Intracellular Staining of pSTAT5 and pS6-Ribosomal Protein in primary human CD8 cells.

Dose-response experiments on primary human $CD8^+$ T cells were performed as described (Ring et al., 2012); in brief, cells were treated with serial dilutions of IL-2, H9, H9-RET,

H9-RETR, then fixed with Phosflow Fix Buffer I at room temperature for 10 min (BD Biosciences), and washed once with flow cytometry buffer. Cells were then permeabilized by slowly adding cold BD PhosflowTM Perm Buffer III and incubated for 30 min on ice. Cells were washed and stained with PE-conjugated anti-STAT5 pY694 (BD Biosciences) or APC-conjugated anti-phospho-S6 ribosomal protein (Ser235/236) (clone D57.2.2E) at room temperature for 30 min in the dark, washed again with flow cytometry buffer, and data acquired on a FACSCanto II flow cytometer (BD Biosciences) and analyzed with FlowJo (Tree Star).

Inhibition of IL-2-induced pSTAT5

Freshly isolated $CD8^+$ T cells and $CD8^+$ T cells pre-activated with anti-CD3 + anti-CD28 were stimulated with IL-2 in the absence or presence of H9-RET or H9-RETR, and pSTAT5 assessed. Cells were incubated with or without anti-Tac or Mikβ1, or H9-RETR-Fc4 for 1 hr, stimulated with a range of doses of IL-2 or IL-15 for 30 min, and pSTAT5 measured by flow cytometry. For NK cell experiments, freshly isolated human NK cells (NK Cell Isolation Kit II, Miltenyi Biotech) were stimulated with serial dilutions of IL-15 in the presence or absence of the indicated IL-2 variant, and pSTAT5 assessed.

Western Blotting

Cells stimulated with or without cytokines were lysed in RIPA buffer containing 1% IGEPAL CA-630 (Sigma). Equal amounts of lysates were resolved on 4 to 12% Bis-Tris NuPAGE gels (Invitrogen), transferred to membranes, and the membranes incubated for 1 h at room temperature with antibodies to pSTAT5(Y694) (Cell Signaling Technology,

Inc., Beverly, MA) or STAT5 (BD Transduction Laboratories, San Diego, CA). Bound antibodies were detected with goat anti-rabbit- IgG (H+L)-HRP conjugate (1:5,000 dilution) and with goat anti-mouse IgG (H+L)-HRP conjugate (1:10,000 dilution) (Biorad). Immunoblots were visualized using enhanced chemiluminescence (ECL, GE healthcare). In some experiments, membranes were reused after incubating in stripping buffer (Millipore) for 15 min at room temperature.

Thymidine incorporation assay

Total human $CD8^+$ T cells were isolated from PBMCs and added to anti-CD3 (2 μg/ml) coated 96-well round bottom plates at 200 μl/well at 10^6 cells/ml with soluble anti-CD28 (1μg/ml) and incubated at 37° C for 3 days. Cells were then washed and rested in complete medium for 1 day, and aliquots of 2×10^3 cells/100 μl/well were plated and incubated for 2 days with varying concentration of IL-2 variants. [^{3}H]-thymidine was added, and 16 hours later cells were harvested and [^{3}H]-thymidine incorporation determined by liquid scintillation.

CFSE Dilution and EdU Proliferation assays

Freshly isolated pre-activated $CD8^+$ T cells (20 x 10^6/ml) were labeled with 2.5 μM CFSE (Molecular Probes) in PBS at room temperature for 7 min, washed once with 100% FBS (2 ml/sample), and then twice in complete RPMI medium. 2 x 10^6/ml. CFSE labeled cells were cultured in the absence or presence of wild type IL-2, H9, H9-RET, H9-RETR, or IL-2 plus H9-RETR. Cell proliferation was assessed by flow cytometric analysis of CFSE dilution at indicated time-points. For EdU proliferation assays, $CD8^+$ T

cells were pre-activated with anti-CD3 + anti-CD28 and cultured as above. 16 h before harvesting, 10 mM EdU was added, cells were stained for surface antigens as indicated, and then for intracellular EdU according to the manufacturer's protocol (BD Biosciences). Cell proliferation was assessed by flow cytometry.

Gene Expression Analysis by RT-PCR

Total RNA was isolated using RNeasy Plus mini kit (Qiagen) and 200 ng was used together with oligo dT (Invitrogen) and the Omniscript reverse transcription kit (Quiagen) to synthesize cDNA. Quantitative RT-PCR was performed with an ABI 7900 HD Sequence Detection System. RT primers and probes were from Applied Biosystems. Expression was normalized to *RPL7*.